



Review Paper

Anti-Wetting Membrane Distillation to Treat High Salinity Wastewater: Review

Jing Yi Chin, Abdul Latif Ahmad, Siew Chun Low*

School of Chemical Engineering, Engineering Campus, Universiti Sains Malaysia, Seri Ampangan, 14300 Nibong Tebal, Pulau Pinang, Malaysia

Article info

Received 2020-06-27
 Revised 2020-08-07
 Accepted 2020-08-16
 Available online 2020-08-23

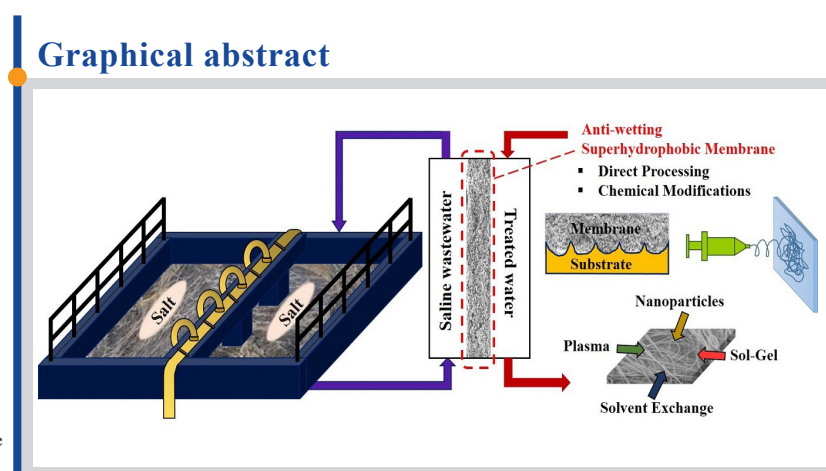
Keywords

Membrane distillation (MD)
 Desalination
 Energy efficiency
 Superhydrophobic modifications
 Aquaculture

Highlights

- MD process to treat various high salinity wastewater
- Energy efficiency evaluation and wetting challenges of MD
- Enhanced superhydrophobicity of the membrane as a solution to the wetting issue
- The prospect of MD process in the treatment of aquaculture wastewater

Graphical abstract



Abstract

Shortage of freshwater supply is now a pressing worldwide stress. While there is plenty of water on this blue planet, a major portion of it is inapt for human use due to its high salt content. A string of desalination technologies was thus presented to convert high salinity water sources into fresh ones. The conventional desalination technologies are capable to perform desalination effectively. Nonetheless, concern like their energy efficiency is put forward. Following that, this review aims to discuss the feasibility of employing membrane distillation (MD), an advanced application that outperforms conventional desalination technologies in terms of its energy efficiency to treat various kinds of high salinity wastewaters. Challenges associated with MD were investigated whereby emphasis was given to membrane pore wetting issue. The latter part of this review focused on resolving MD's challenges via synthesis of superhydrophobic membranes by inducing surface roughness and lowering surface energy of neat membranes. Various fabrication materials and modification methods such as direct manufacturing and addition of extrinsic additives to produce anti-wetting membrane were scrutinized. The superhydrophobic modification techniques include incorporation of nanoparticles, solvent exchange and plasma treatment, have successfully brought up the static contact angle of modified membranes to 150-173°. Those techniques resulted in enhanced permeate flow, with rejection of undesired component close to 100%. In short, MD demonstrates superiorities with regards to its thermal efficiency and stable desalting performances. MD also sees potentials in treating saline effluent from aquaculture, an imperative industry developed aggressively recently to bridge global food supply and demand.

© 2020 MPRL. All rights reserved.

Contents

| | |
|--|-----|
| 1. Introduction..... | 402 |
| 2. Membrane distillation: configurations and applications..... | 402 |
| 2.1. Energy consumption of membrane distillation..... | 402 |
| 2.2. Challenges of MD applications: membrane perspective..... | 405 |
| 3. Superhydrophobic membrane..... | 406 |
| 3.1. Membrane materials of MD..... | 407 |
| 3.2. Direct processing techniques to induce membrane hydrophobicity..... | 408 |
| 3.2.1. Electrospinning..... | 408 |
| 3.2.2. Nanoparticles..... | 409 |
| 3.2.3. Induced surface roughening upon membrane fabrication..... | 409 |
| 3.3. Superhydrophobic membrane enhancement through chemical modifications..... | 409 |

* Corresponding author: chsclow@usm.my (S.C. Low)

| | |
|---|-----|
| 3.3.1. Plasma treatment..... | 409 |
| 3.3.2. Solvent Exchange..... | 410 |
| 3.3.3. Sol-Gel..... | 410 |
| 4. Future prospects and directions of MD..... | 410 |
| 5. Conclusion..... | 411 |
| References..... | 411 |

1. Introduction

By 2025, half of the world's population will suffer from extreme water scarcity in their living area, according to the World Health Organization (WHO). While the earth is 75% covered by water, only 2.5% of it is freshwater and is consumable. To transform the remaining 97.5% of water comprising high salt content (seawater) into freshwater, numerous conventional desalination technologies, for instance reverse osmosis (RO) and multi-stage flash (MSF) [1] were embraced. Apart from seawater, treatment of high salinity wastewater such as brine water from RO [2], refractory seafood processing wastewater [3], textile wastewater [4], effluent produced from shale gas extraction [5] and many more is equally important, to be recycled for further usage, to reduce stress on clean water supply, also to minimize adverse impacts towards the environment.

The widely used conventional desalination technologies (RO and MSF) are proven to desalt saline wastewater effectively [6,7]. However, their efficacies are compromised by membrane fouling and high energy consumption issues [1]. On top of this, substantive and paramount of researches were put forth to introduce membrane distillation (MD) as a feasible desalination technology, considering its advantages over its counterparts. As MD is thermally driven and nil pressure [8] is applied to the operation, possibility of fouling is therefore minimized as compared to pressure driven membrane applications. Furthermore, there are attainable solutions to cope high thermal energy consumption of MD, whereby energy needed to operate MD can be generated from low grade energies sources [9]. Improvement of MD's thermal efficiency on the other hand, can be realized through system hybridizations [10] and operational tunings [11-13].

Membrane distillation operations however, associate with membrane wetting challenges that greatly prone to jeopardising its separation functionalities [14]. Therefore, fabrication of anti-wetting membranes for MD is premier to retain and sustain MD's performances. Creations of anti-wetting membrane surfaces involved concerted efforts to render the membranes superhydrophobic, a state at which surfaces of membranes repel water excellently. Superhydrophobic modifications of membranes can be executed chemically [15-17] or physically [18,19], with mutual aims to increase surface roughness while lowering surface energy of the modified membranes [20]. While chemical modifications were accomplished by altering surface properties of the membranes, physical modifications were implemented by inducing micro to nanoscale surface roughness upon fabrication of membranes. A work by Teoh et al. [21] showed that by imprinting hierarchical 3D-microtexture on PVDF membrane surface during membrane synthesis, the membrane surface was rendered superhydrophobic with static contact angle of 156°. The micro-scale patterned surface also enhanced dynamic wetting behaviour of the membrane by bringing down sliding angle to 5° and improved direct contact MD permeate flux up to 24 kg/m²h.

In view of the pronounced necessity to establish a well-rounded desalination system to abate water stress globally, the objective of this paper is to comprehensively review the practicability of the deployment of MD as a desalination technology. This review summarizes applications and performances of MD to treat various types of high salinity wastewaters, as of to provide backgrounds of MD's energy consumption, challenges faced and the mitigations, as well as the future prospects of MD in desalinating saline wastewaters, e.g. aquaculture wastewater.

2. Membrane distillation: configurations and applications

Membrane, a selective barrier has gained elevating popularity in separation applications in vast varieties of industries, like retention of heavy metal [22], pharmaceutical products purification, oil/water separation [23], immunoassay [24], food and beverage industry, to name a few [15,19]. Pressure driven membranes in common, suffer from high fouling potential and high equipment cost, which subsequently compromise economic aspect of the separation processes. As compared to pressure driven membranes, MD has better prospects to be freed from their associated challenges as the main benefits of MD system is that it can operate under atmospheric pressure feed and is easily scalable [8] Hence, MD emerges as an attainable solution, considering its workability at very low or nil pressure gradient and it is

possible to integrate waste heat into the system to power the operation. Low surface energy of hydrophobic MD membranes also reduces chances of crystal nucleation, thus lowering possibility of fouling. Process of membrane distillation is driven thermally, whereby it consists a hydrophobic porous membrane as the major separation component. The hot (feed) and cold (permeate) streams will be circulated on both separated sides of the membrane, generating vapour pressure gradient due to temperature discrepancy. During operation, water vaporizes from the hot feed and diffuse across the membrane to the cold permeate. The water vapours then condensed in the flowing cold permeate stream and are collected as pure water, leaving non-volatile constituent in the hot retentate stream [8,9].

However, there are many factors affecting MD performances, for instance vapour collection methods, module designs and operating parameters which include temperature gradient between feed and permeate, salinity and foulants present in feed. On top of that, morphology, chemical/physical characteristics and surface wettability of the membranes also play crucial roles, whereby the MD flux can be significantly improved upon optimization of the resistance across the porous structure [25,26]. There are various configurations of MD that are capable to treat high salinity wastewaters (Figure 1), including direct contact (DC) MD, air gap (AG) MD, sweeping gas (SG) MD and vacuum (V) MD, depending on their mechanisms to generate vapour pressure gradient between feed and permeate streams. Generally, heat and mass transfer across the separation components (membrane and air gap) of MD are critical factors that contribute to each configuration's pros and cons, as summarized in Table 1.

Applications of different configurations of MD extend across a broad varieties of separation processes, especially in treating high salinity wastewaters as listed in Table 2. Besides, MD demonstrates high potential in treating wastewater containing phosphorus and nitrogenous wastes. Kim et al. [33] treated digestate of livestock wastewater that contained high concentrations of organic matters, total nitrogen, ammonium nitrogen, total phosphorus and phosphate with a 72 hr DCMD process. After the DCMD treatment, >99% of phosphorus, 84.7-95.9% of total nitrogen and 89.1-92.6% of ammonia were successfully rejected from the wastewater. In another work by Boubakri et al. [34], a 99.9% nitrate rejection rate was achieved in DCMD experimental run using both PVDF (Flux: 37.21 L/m² h) and PP (Flux: 4.12 L/m² h) membranes. The deployment of VMD and modified DCMD to remove ammonia from its aqueous solution can be seen in El-Bourawi et al. [35] and Qu et al.'s [36] works. The former attained removal efficiencies of over 90% with separation factors higher than 8 while the latter was able to remove 99.5% of ammonia from the separation process.

2.1. Energy consumption of membrane distillation

The MD's energy efficiency and flux performances are strongly governed by concentration polarization, temperature gradient as well as operation conditions (e.g. difference of temperature between feed and permeate, circulation flow rate, and etc). Since MD process is thermally driven, thermal efficiency, a subset of energy efficiency will be the main focus in the following discussion. Heat lost during vaporization and heat conduction through separation units are usually the key factors contributing to low thermal efficiency of MD, which ranged from a mere 20 to 30% in general [12]. As discussed by Ullah et al. [1], the conventional desalination technology: multi-stage flash (MSF) operated at thermal energy of 53-70 kWh/m³ and its recovery rate is very low, ranging from 15-20%. Reverse osmosis (RO) then appeared as an improved technology in terms of recovery rate (30-50%) with zero thermal energy required. However, RO has relatively high electrical energy requirement. In fact, the energy consumption of RO increases with increased feed salinity. This is because a higher hydraulic pressure must be applied to separate fresh water from high salinity feed which possesses high osmotic pressure [51]. To cater drawbacks of both MSF and RO, membrane distillation was introduced. MD pleasantly showed satisfactory recovery rate at 60-80% and consumed minor electrical energy at 1.5-3.65 kWh/m³ compares to MSF. Nonetheless, its thermal energy requirement is the highest among them all.

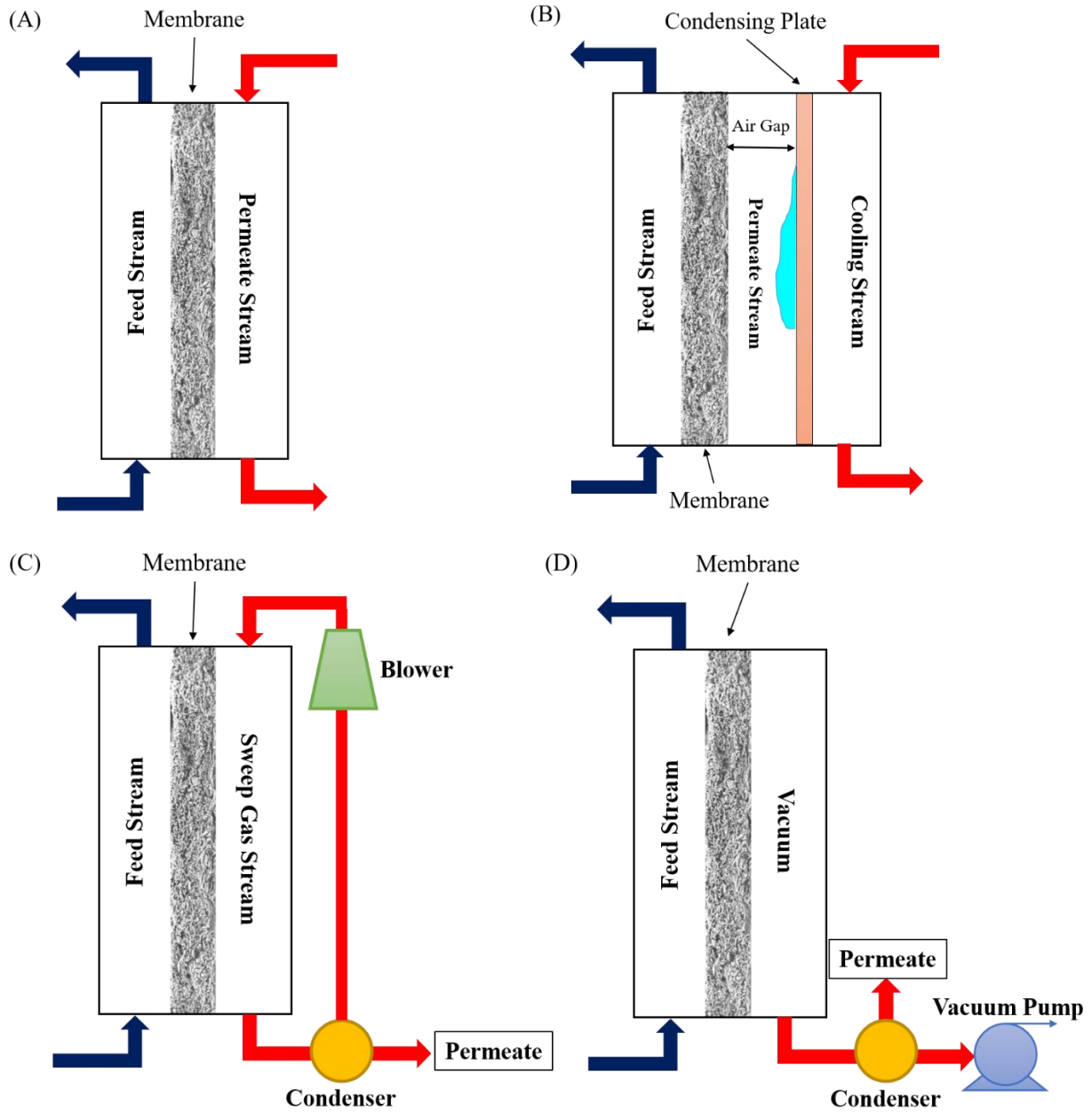


Fig. 1. Illustration of operating concepts of (A) DCMD (B) AGMD (C) SGMD (D) VMD.

Table 1
Advantages and drawbacks of each MD configuration [1,8,14,27-32].

| MD Configurations | Advantages | Drawbacks |
|-------------------|---|---|
| DCMD | Good salt rejection, high permeate flux, huge operating temperatures range from 5 to 130 °C. | Significant loss of heat because of the high thermal conduction across the membrane. |
| AGMD | High thermal efficiency because of the presence of air gap that minimize heat lost. It allows recovery of latent heat. | Huge thermal and mass transfer resistances due to existence of relatively thick air gap compared to thickness of the polymeric membrane. |
| SGMD | Presence of sweeping gas improved mass transfer at the permeate side, while maintaining low thermal conduction and high thermal efficiency. | Complex process because it requires high volume of inert gas to sweep the water vapour at the membrane permeate (cold side) before condensing it using a large condenser. |
| VMD | Best flux performance contributed by astonished enhancement of mechanical pressure difference between the permeate and feed. | High possibility to wet the membrane because of the reduced pressure at the membrane permeate. |

Table 2
Overview of published results for desalination applications of MD processes.

| MD Config. | Feed Constituent | Membranes | | | | Feed/Permeate/Coolant T _f , T _p /T _p /T _c (°C) Vacuum P, p _v (kPa) | Feed/Permeate/Coolant Flow Rate, F _f /F _p /F _c (L/min) | MD Durations (hr) | Flux (kg/m ² h) | Salt Rejection (%) | Ref. |
|------------|--|-----------------------------|----------------|--------------|------------------|---|---|----------------------|-------------------------------|-----------------------|------|
| | | Based Materials, Categories | Thickness (μm) | Porosity (%) | Hydrophobicity | | | | | | |
| DCMD | 30 g/L NaCl aqueous solution | PSU, polymeric | 97.1 | - | Superhydrophobic | T _f : 70 T _p : 20 | F _f : 0.6 F _p : 0.4 | 12 | 21.5 | >99.99 | [37] |
| | Actual RO brine containing high and organic and inorganic ions | PVDF, polymeric | 55 | 57 | Superhydrophobic | T _f : 70 T _p : 25 | F _f /F _p : 0.75 | 21 | 40.5 | 99.98 | [2] |
| | Real seawater | PVDF, polymeric | 99.9 | 63.8 | Superhydrophobic | T _f : 70 T _p : 28 | F _f : 3.2 F _p : 6.4 | 120 | 2.78 | 99.9 | [38] |
| | 30 g/L NaCl aqueous solution and 10 mg/L humic acid | Mullite, ceramic | - | 57 | Omniphobic | T _f : 65 T _p : 20 | - | 8.3 | 4.32 | >99.99 | [39] |
| | Oil saline solution with 1000 ppm crude oil and 35 g/L NaCl | PVDF-HFP, polymeric | - | - | Omniphobic | T _f : 60 T _p : 20 | F _f : 0.45 F _p : 0.2 | 6 | Normalized: 1.0 | >99.99 | [40] |
| AGMD | 3.5 wt% NaCl | PH, polymeric | 100 | 88.7 | Superhydrophobic | T _f : 60 T _c : 20 | F _f /F _c : 0.2 | 60 | 22.9 | 100 | [41] |
| | 0-6.5 wt% NaCl solution | Alumina, ceramic | 181 | 57 | Superhydrophobic | T _f : 80 T _c : 20 | F _f : 0.58 | - | 33.0-30.6 | >99.8 | [42] |
| | 0.5 M NaCl solution | Zirconia, ceramic | 310 | - | Superhydrophobic | T _f : 75-95 T _c : 5 | F _f : 6.7 F _c : 0.83 | 6 | 5.4-9.4 | >99.5 | [43] |
| SGMD | 20 wt% salt solution | α-Silicon Nitride, ceramic | - | 65 | Superhydrophobic | T _f : 90 | F _f : 1.7 | 500 | 8.09 | >99.9 | [44] |
| | 4-12 wt% salt solution | α-Silicon Nitride, ceramic | - | 57 | Hydrophobic | T _f : 75 T _p : 25 | F _f : 1.7 | - | 11.75-9.19 | 99.99 | [45] |
| VMD | 35 g/L NaCl aqueous solution | PTFE, polymeric | 120 | 75 | Superhydrophobic | T _f : 65 p _v : 97 | F _f : 1.84 | 3 | 52.6 | 99.2 | [46] |
| | Real seawater | PP, polymeric | - | 65 | Superhydrophobic | T _f : 70 p _v : 95 | F _f : 0.5 | 100 | 31.2 | >99.95 | [47] |
| | 35 g/L NaCl aqueous solution | PVDF, polymeric | - | 55 | Superhydrophobic | T _f : 27 p _v : 94.8 | - | 6 | 2.9 | 99.98 | [48] |
| | 3.5 wt% NaCl | PVDF, polymeric | 101 | 70.2 | Superhydrophobic | T _f : 80 p _v : 3 | F _f : 0.13 | 26 | 28.4 | >99.9 | [49] |
| | 30 g/L NaCl aqueous solution | Alumina, ceramic | 220 | 35 | Superhydrophobic | T _f : 55-75 p _v : 5 | F _f : 2.7 | 20 | 30 | 99.9 | [50] |

Abbreviations: Config, Configurations; T, Temperature; P, Pressure; PSU, Polysulfone; PVDF, Polyvinylidene fluoride; PVDF-HFP, Poly(vinylidene fluoride)-co-hexafluoropropylene; PH, polyvinylidene fluoride-co-hexafluoropropylene; PTFE, Polytetrafluoroethylene; PP, Polypropylene

Though there's still big rooms of improvement for MD's thermal efficiency, it remains as researchers' fond in progress to perfect desalination technologies. Reasons being MD is advantageous over its kind in some other aspects and there are available solutions for its high thermal energy consumption. Several research works have succeeded to achieve MD process with thermal efficiency as high as 92-95% [13,52], demonstrating noteworthy ameliorations in MD applications. Conversely, in MSF, almost 67% of the total energy consumed will be rejected as waste heat [1], while the least energy consumed process-RO, has high tendency to suffer from clogging of minerals on membrane due to its high operational pressure at 55 - 80 bar for seawater desalination [53]. In this case, MD holds opportunities to counter issues faced by MSF and RO. One key supporting factor of MD being a prominent energy efficient purification technology is its ability to replace the thermal energy required with low grade heat resources, including geothermal energy, solar energy, wind, tidal, nuclear energy or low-temperature industrial streams [9]. Potential of MD is further extended to its comparatively higher compactness than conventional desalination technologies, rendering it a superior small scale and off grid purification technology [19]. Besides, MD has the ability to reject nearly 100% of non-volatile solute, does not affect by feed salt concentration and operates at low hydrostatic pressure [54].

On the downside, MD is subjected to relatively higher operational cost issue. There is study that states solar-powered MD imposed higher operation cost as compared to photovoltaic-powered RO [1]. Similarly, in another work, the leveled cost of water (LCOW) for the two desalination technologies was compared by Ahmed et al. [55]. The LCOW of SWRO and solar-powered MD were \$1.25 and \$5-85 respectively per cubic meter water. Karanikola et al. [28] simulated the optimal thermal desalination systems using different MD configurations via MATLAB to unravel their respective economic performances. The salinity of initial feed used in the process was 3.5%. The total present value cost, including equipment and operational cost have been processed annually for a 20-year of design duration at 5% of discount operator. The simulation results showed that the total present value (TPV) cost ranged from 14.3 to 21 US dollar per cubic meter of treated water, depends on different configurations. From the simulation, it was also concluded that solar thermal collectors contributed to the largest portion of the total cost for all MD systems, i.e. an approximate quarter of the TPV cost. This economical evaluation deduced that cost reduction can be realized by making modifications on processes that will improve efficiency of production or usage of thermal energy. Following that, several MD process intensification initiatives (Table 3) were implemented and the results showed parallelism to Karanikola et al.'s findings.

Other than process intensifications and integrations, some researchers focused on tuning existing operational parameters to improve energy efficiency of MD. The definition of energy efficiency of MD is termed as the ratio of the latent heat of vaporization to the total heat (conduction and latent heat). Heat crosses membrane as latent heat via mass transfer will induce flux production, whereas conduction of heat has nil contribution towards increment of flux, hence considering as heat lost [12]. To enhance thermal efficiency of MD, system parameters have to be adjusted so as to maximize the latent heat while minimizing the conduction heat passing through the membrane. Several parameters were studied with aim to improve membrane thermal efficiency (MTE) and were proven to be effective. First, to fabricate membrane with low thermal conductivity materials (e.g. PTFE, PP, PVDF). When Al-Obaidani [11] performed MD with membranes of thermal conductivity expanded from 0.05 to 0.5 W/mK, it was found that thermal efficiency and transmembrane flux decreased by 55% and 26% respectively.

Second, by optimizing thickness of membrane, porosity and the average pore radius (r) [12]. A thin membrane could minimize mass transfer resistance, but further decrement in membrane thickness leads to increased heat loss through conduction, consequently decreasing the temperature difference across the membrane, thus reducing driving force and water permeation. While highly porous membrane is beneficial to promote higher flux, one should take note on the membrane pore size selection. The membrane pores need to be small to prevent wetting, but large enough to increase flux, whereby the ideal membrane pore sizes lie between 300 to 400 nm. Moreover, a crucial factor to prevent membrane wetting in order to maintain high functionality of MD is to fabricate membranes with hydrophobic materials which effectively hinder liquid of both feed and permeate sides from crossing over the separation barrier. Third, to increase feed temperature, which in turn increases vapour partial pressure difference across the membrane. This trend is agreed by an experimental work conducted by Fan and Peng [13] using a flat sheet PVDF membrane of 78% porosity synthesised via combination of vapour induced phase separation and double layer casting process. With salt solution of 35 g/L concentration used as feed, the permeate of DCMD with effective membrane area of $26.4 \times 10^{-4} \text{ m}^2$ increased nearly 5 times, achieving approximately $33 \text{ kg/m}^2 \text{ h}$ when the temperature of feed varied from 50 to 85 °C at a flow rate of 0.9 L/min. Furthermore, from the same study [13], it was reported that vapour flux was enhanced with increment of flow rate of cold permeate and hot feed, both from 0.225 to 2.7 L/min, with the hot side's flow rate imposed a higher effects compared to the cold side. When flow rate increases, a higher circulation velocity was promoted, inducing a more vigorous flow mixing across thermal boundary layers [59]. The enhanced hydrodynamic conditions which favoured the turbulent flow regime will lead to thinning of thermal boundary layers hence reducing effect of concentration polarization [60]. Again, optimization of flow rate should be taken into consideration. While high flow rate is beneficial to decrease membrane polarization effect, it generates high pressure that can lead to membrane wetting [12].

2.2 Challenges of MD Applications: Membrane Perspective

While the high thermal consumption can be mitigated by harnessing alternative energy sources and adjusting process parameters as described in section 2.1, MD suffers from other drawbacks such as wetting, scaling, fouling, concentration and temperature polarizations [61]. Moreover, the application of MD in seawater desalination has possibilities of scale formation and organic matter accumulation on the membrane surface, altering its hydrophobicity, which then induces liquid intrusion into pores, causing dwindling and deterioration of permeate flux and quality [14]. On the other hand, foulants such as precipitations of organic and inorganic matter can clog membrane pores, which reduce the membrane's permeability [27].

All the drawbacks mentioned are interrelated, nevertheless, emphasis is given to membrane pore wetting, a unique and the most significant technical challenge of MD. Wetting happens when liquid feed penetrates through the membrane pores, which then leads to unacceptable salt rejection [62]. The primary cause of membrane pore wetting is fouling, and the list extends to the presence of surfactants in feed which reduce the surface tension of the solution, capillary condensation and membrane damage. Besides, pore wetting also happens when the hydraulic transmembrane pressure surpasses the liquid entry pressure (LEP) of the membrane. The membrane could be wetted under four conditions: non-wetted, surface-wetted, partially-wetted, and fully-wetted.

Table 3
Process specifications and operational improvements of MD applications with ameliorated thermal efficiency.

| MD Applications | Process Specifications | Operational Improvements | Ref. |
|---|--|---|------|
| Solar energy integrated MD | Solar absorbing area of 1.6 m ² and membrane area of ~0.2 m ² with high salinity solution of 35 ppt (e.g. seawater) as feed | With flux of 4 to 10 L/m ² h, ~3-5 L of drinkable water and 2.5 - 6 kWh of heat energy can be harvested from the system per day | [56] |
| Zero thermal energy input membrane distillation | No preheating needed and no production of waste. Temperature difference presents naturally between the water at sea surface (30 °C) and sea bottom (10 °C) | Low specific energy consumption of ~450 Wh/m ³ based on simulation results | [1] |
| Integrated AGMD-DCMD system | Able to treat feeds at low temperature (40 °C), and simultaneously treat two types of feed at their respective desired operating temperatures | Compare to stand alone DCMD system, it consumed ~40% lower specific thermal energy, increased gained output ratio (GOR) by ~67% and produced 4 times higher of permeate | [57] |
| Memstill® | A patented MD internal heat recovery process, reduced operation cost through heat recoveries from condensation to preheat the cold feed | Able to treat water at lower cost (\$0.26/m ³) than RO (\$0.45/m ³) when operated at 50% recovery rate, consumed only 73.75 MJ/m ³ of energy (half of MSF) as it utilized low grade heat | [58] |

Non-wetted (Figure 2A) is a wetting level where a convex meniscus is formed at the membrane pores (liquid-membrane interface) that impedes entering of liquid into membrane's void, as described by Rezaei et al. [63]. This phenomenon occurred when membrane-liquid adhesive forces are weaker than the cohesive forces within the liquid (high surface tension of the liquid), leading to a desired low water sliding angle. Supported by Seyed Shahabadi et al.'s research [64], the plus point of non-wetted state was further described. Their original polyvinylidene fluoride-co-hexafluoropropylene (PH) electrospun membrane demonstrated WCA as high as $142 \pm 4.3^\circ$. However, despite of the high contact angle, water droplet still strongly adhered to membrane surface, even after the membrane was turned upside down during sliding angle analysis. On the other hand, the modified dual layers TiO_2/PH membranes ($\text{WCA} > 155^\circ$) have significantly lower sliding angles at a range below 20° . When tested with DCMD for 24 h, the permeate quality of original PH membrane easily deteriorated after 8 h due to wetting (extremely low salt rejection) while the modified membrane maintained high flux and salt rejection throughout the whole MD process. Extended from this result, it is safe to infer that due to MD's operating mechanism in which only vapours will be transferred through the pores of membrane, it is of utter importance for the membrane pores to remain dry. First, to provide sufficient effective interface area for vaporization; second, to impede passing through of undesired non-volatile constituents from feed to permeate stream via wetted pores.

When the membrane experienced surface-wetting (Figure 2B), liquid/vapour interface shifted inward of membrane cross-section, decreasing effective area for vaporization. Temperature polarization occurs, causing gradual decline of permeate flux. This phenomenon was observed by Ray et al. [65] in which the water flux of modified superhydrophobic PP mat ($\text{WCA}: 163^\circ$) declined by approximately 10% over 16 h of MD operation. When the membrane's surface is wetted, local solute concentrations and scale formation rate elevate, attributed to crystal growth inside pores. This will inhibit diffusion of solutes between the feed bulk and the wetted pores. Conversely, temporary flux increment might be observed under certain conditions, for example, when vapour transferred faster through the dry area of pore as the diffusion path is shorten.

In Figure 2C, the partially-wetted occurred as feed liquid infiltrates deeper into membrane pores. Two conditions might happen, permeate flux declines as the active surface area for mass transport reduced, or increase of permeate flux as liquid transport overtakes vapour transfer followed by a plunge owing to pores blockage by foulants [63]. At this point, 'water bridges' are generated, allowing passage of salts to the permeate side, which jeopardises permeate quality [66]. From the same work of Ray et al. [65], the severity of membrane wetting on permeate quality was further highlighted when the partially-wetted neat PP mat was compared with the superhydrophobic modified membranes that only wet on the surface. The neat PP mat (LEP: 0.3 bar) could only maintain a salt rejection rate of 96-97%, while the modified membrane (LEP: 4.96 bar) was able to achieve 99-100% salt rejection throughout the separation process. As the wetting worsened, MD process is incapacitated. The MD membrane would no longer acts as a separation barrier as feed solution flows through the membrane pores at fully-wetted stage (Figure 2D).

Warsinger et al. [67] proposed several strategies to mitigate membrane pore wetting challenge. A few effective strategies include pH control of MD feed, thermal water softening and tailoring membrane properties by rendering it superhydrophobic or adjusting its surface porosity were introduced. The previous two mitigations suffer from certain disadvantages such as acidifying of the feed solution and the necessity of boiling as an expensive pre-treatment in terms of energy. Moreover, sustainability of these two methods is in doubt as their functionalities could only be extended to certain applications. For example, the workability of pH adjustment approach was type of feed dependent. At pH of 4, calcium carbonate scale could be effectively removed but prevention of silica scale failed at this acidity level. Moreover, pH modification of a solution could be profoundly expensive, which hinders the comprehensiveness of its applicability in vast areas. On the other hand, while thermal water softening succeeded in lowering declination of flux (from 12% to 3% of flux reduction) when purifying feed containing bicarbonate ion (HCO_3^-), it on the contrary worsened the wetting condition in an effort to treat tap water containing an even lower concentration of HCO_3^- [68].

Besides the strategies proposed, some researchers ventured into fabricating omniphobic membranes to cope with the membrane wetting phenomenon. In an effort to treat saline feed containing sodium dodecyl sulfate (SDS), Wu et al. [69] rendered an electrospun PVDF-HFP membrane omniphobic by means of fluorination using 1H, 1H, 2H, 2H-perfluorodecyltrichlorosilane. The resultant membrane exhibited stable flux over 8 hr DCMD test, excellent anti-wetting properties and was able to withstand harsh situations like ultrasonic, boiling water, acid and base treatment. Despite demonstrating commendable anti-wetting performance, usage of omniphobic membranes is popular mainly in niche applications to treat saline wastewater containing oily and complex components such as oily seawater [70], coking wastewater [71] and RO brine from coal seam gas water [72]. Thus in this review, focus is given to address the membrane pore wetting issue through the widely adopted solution: superhydrophobic modifications, considering its efficacy and sustainability in desalination processes.

3. Superhydrophobic membrane

Conventional definition for superhydrophobic is when a surface has high static contact angle ($>150^\circ$) and low sliding angle ($<10^\circ$) [25]. The anti-wetting mechanism of a surface can be explained through Cassie-Baxter model, as illustrated in Figure 3, whereby the water repellent properties are influenced by combined impacts of low surface energy material and surface roughness [20]. When a surface is rough, spaces between micro structures formed air pockets that induced solid-air interface, hampering direct seeping of liquid through membrane pores. Surface roughness also promotes tortuosity of three-phase (solid-liquid-air) interface lines and lowers liquid pinning effects, which governed a surface's ability to repel water and self-cleaning properties [73]. Meanwhile, low surface energy membrane materials induced low adhesion of water droplet onto membranes' surfaces, which enhance the superhydrophobic properties a membrane [74].

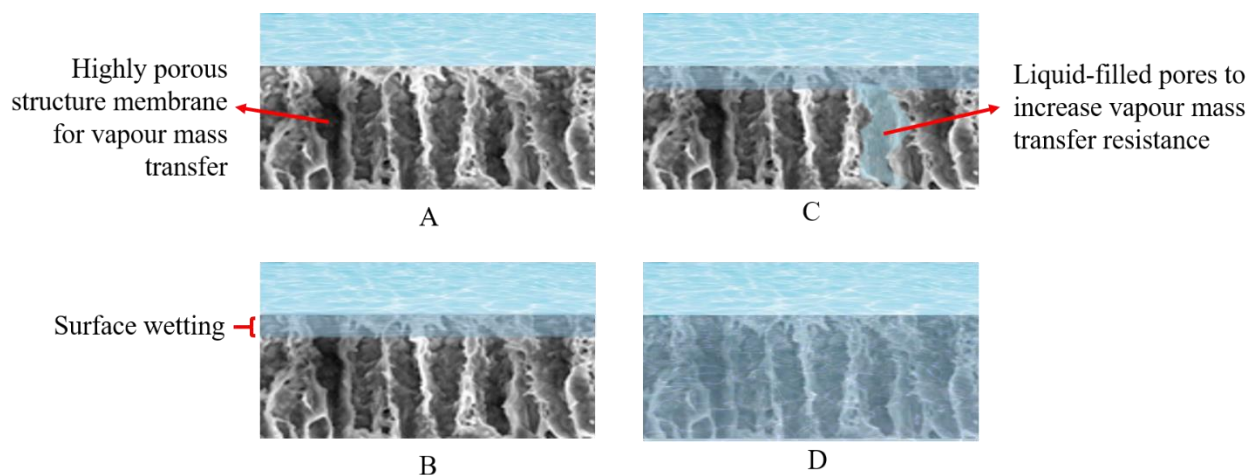


Fig. 2. (A) Non-wetting, (B) Surface-wetting, (C) Partial-wetting, (D) Full-wetting of MD membrane.

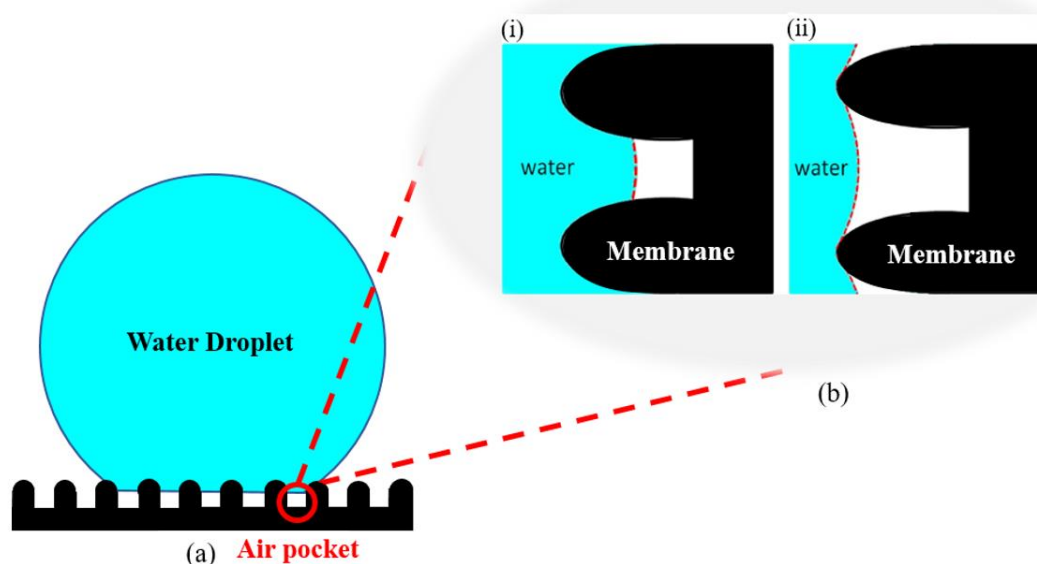


Fig. 3. (a) Cassie-Baxter model (b) Schematic illustration of gas-liquid interfaces of (i) hydrophobic (ii) superhydrophobic membranes.

For MD, the installed membrane should have high porosity and the lowest heat conduction possible [75]. In addition, since only volatile water vapours are allowed to pass through the separation boundary in MD processes, it is crucial to prevent the direct-contacting feed liquid from penetrating into membrane pores. Thus, superhydrophobic nature of MD membrane is highly preferable in this case as it hinders entering of feed liquid into the membrane pores owing to surface tension of the feed liquid [10]. As illustrated in Figure 3 (b), the red dotted line denoted interface of membrane, water and air. If the membrane is hydrophobic (contact angle higher than 90° but less than 150°), the air-pocket area of membrane-water-air interface is smaller (Figure 3 (b-i)). Meanwhile, for a superhydrophobic membrane, the 'lift up' effect is expected, which increases the effective membrane-water-air interface area (Figure 3 (b-ii)) for vaporization of water molecules, thereby enhancing MD flux [15].

Zooming into relationship between surface roughness and membrane's superhydrophobicity based on the Cassie-Baxter model, it is proven that the two underlying decisive factors that give rise to superhydrophobicity are: i) sizes and ii) evenness of the roughness creators on the membrane surface [73]. Tiny and regularly arrayed rough structure trapped air more efficiently, leading to small actual contact area between liquid and membrane surface. It is also worth mentioning that as the scale of roughness decreases, the contact angle will increase, attributing to increment of cavities ratio on the rough surface. A relevant example demonstrated by Wang et al. [73] revealed that an electrospun membrane, having roughness induced by micro-meter PVDF beads could only achieve contact angle close to superhydrophobic (145.6°). This is because the surface is not rough enough for air to be trapped effectively in the apertures. The area of contact between the water droplet and electrospun membrane is correspondingly large in this case. However, when SiO_2 particles modified with epoxy-siloxane were coated on the PVDF electrospun membrane, contact angle of the modified membrane improved considerably, reaching superhydrophobic state. The contact angle enhancement was also seen to be in relative to the increment of weight ratio of SiO_2 additives/PVDF, to a maximum of 5:1 (WCA: 161.2°).

Plenty of researches had been conducted and implemented to synthesize superhydrophobic membranes. The efforts ranged from producing membranes from anti-wetting materials, to membrane surface modifications that render them superhydrophobic. Depends on the membrane materials and preparation procedures, different modification methods could be embraced, commonly through direct processing to induce a rough membrane surface morphology or/and hydrophobication with aid of additives during membrane casting.

3.1. Membrane Materials of MD

In general, porosity, pore size and thickness of membrane used ranged from 0.60 to 0.95, 0.2 to $1.0 \mu\text{m}$ and 0.04 to 0.25 mm, respectively [27].

Synthesis of MD membranes involved both ceramic and polymeric based materials. Ceramic membranes have porous structures, and stand out for their high thermal and chemical stabilities, which are advantageous for MD applications [76]. The first research of employing ceramic membranes in MD was conducted by Larbot et al. [77]. In the research, both hydrophilic zirconia and alumina based tubular membranes were first modified with grafting method utilizing fluoroalkylsilane solutions to render them hydrophobic before evaluating their MD performances. When tested on MD with 1 M NaCl solution, the alumina membrane exhibited better result with recorded flux of $10.8 \text{ L/m}^2 \text{ h}$ and nearly perfect salt rejection at a feed-permeate temperature difference of 90°C . Also utilizing alumina as based material for hollow fiber membrane, Fang et al. [78] tested the membrane performance in VMD with 4 wt% NaCl as feed at 80°C and imposed a 0.04 bar vacuum pressure to the lumen side of the fiber. As a result, a permeate flux of $42.9 \text{ L/m}^2 \text{ h}$ and salt rejection over 99.5% were successfully achieved. Though proven to be effective to be used in MD to perform desalination process, researches employing hydrophobic ceramic membranes in MD (20% of researches) are relatively scarce as compared to hydrophobic polymeric membranes (80% of researches) [79]. This is mainly due to expensive production cost, low area to volume ratio and brittleness of ceramic membranes that compromise their advantages [80].

Polymeric materials such as poly(propylene) (PP), poly(tetrafluoroethylene) (PTFE), polyethylene (PE) and poly(vinylidene fluoride) (PVDF) are commonly used materials to fabricate MD membranes. These polymers are hydrophobic in nature. Figure 4 summaries available researches in Scopis relating to these polymeric materials to fabricate hydrophobic membranes in the latest five years (2015 to 2020) and their respective characteristics adapted from Wang et al. [10]. As evidenced by the lowest surface energy among other polymers (Figure 4), PTFE possesses the highest hydrophobicity. It also enjoys benefits of good oxidation resistance as well as good chemical and thermal stability. These advantages are however, compromised by great heat conduction through PTFE membranes as it has the highest thermal conductivity [27].

Membrane fabrication technique varied depends on the nature of polymer [30], through thermally or non-solvent phase inversion, melt extrusion stretching, sintering and electrospinning [10]. Details of the processing techniques will be discussed later in section 3.2. As PTFE is a non-polar polymer, it can hardly embrace the common phase inversion fabrication method. Thus PTFE membranes are usually produced through sintering or melt-extrusion processes [10]. In a membrane distillation study, Dong et al. [81] varied PTFE content in membrane fabrication solutions from 0-12 wt.%, resulting transformation of membrane anti-wetting property from hydrophobic to superhydrophobic state. PVDF, a semi-crystalline polymer, on the other hand, is versatile as it can be dissolved in common solvents and be prepared with different methods to obtain various pore structures. Good hydrophobicity and high thermal resistance are among the superior properties

of PVDF [27]. Meanwhile, PP has highly crystalline structure. It outperforms other polymer with its hard elastic properties and relatively lower manufacturing costs. Fabrication of PP membrane involves melt-extrusion stretching, thermally phase inversion and electrospinning process. Superhydrophobic modified PP membrane exhibited excellent anti-wetting abilities and stable flux, although under high salinity feed solution and low feed flow rate for MD process, as investigated by Shao et al. [82]. However, PP's performance in MD applications is limited by its symmetric molecular structure and moderate thermal stability at high temperature [10]. PE is an odourless and non-toxic semi-crystalline polymer with excellent electrical insulation, good acid and alkali corrosion resistance. However, PE has relatively low melting point (around 120 °C) and temperature resistance. Suitable methods to prepare PE membranes are melt-spinning and cold-stretching [83].

3.2. Direct processing techniques to induce membrane hydrophobicity

Hydrophobicity enhancement of membrane can be realized at stage as early as during membrane casting. Common techniques often induce membrane roughness through patterned surface or to incorporate additives into membrane dope solutions.

3.2.1. Electrospinning

A variety of polymers can be used for preparation of smooth nanofibers. Electrospinning is a membrane fabrication technique whereby nanofibers from polymer solution are generated in a high electric field. Membranes fabricated through electrospinning show advantageous properties over traditionally phase inversion made membranes. For instances, thickness of electrospun membrane can be tailor-made, porosity is higher and has better permeability attributed to the interconnected open pore structure. The surface morphology and arrangement of electrospun product are immensely governed by properties of casting solution and the respective fabricating conditions [84-86]. Nevertheless, electrospinning faces challenge of incompetence to be a stand-alone superhydrophobic modification technique. This is because though cross-linked nanofibers provide certain degree of surface roughness as a whole, a booster for hydrophobicity is needed as membranes produced from pure polymer dope solution are usually incapable to achieve superhydrophobicity. Reason being when scoping down to micro or nanoscale, each individual nanofiber formed is actually uniform and smooth when there is no incorporation of hydrophobic additives [81].

To render electrospun membrane superhydrophobic, multitude of efforts had been put forward. Functionalization of nanofibers can be realized in two ways, one being addition of hydrophobic materials directly into the spinning dope solution, whereby the functionalizing materials are embedded into the

matrix of nanofiber; second being post-spinning functionalization in which only the surface is modified [85]. Maab et al. [87] synthesized fluorinated polytriazole (F-PT) and polyoxadiazole (F-POD) electrospun membranes that possessed higher porosity and bigger pores than their phase inversion fabricated counterparts. F-PT achieved a water static contact angle of 162° and the highest water permeate of 85 L/m²h with salt rejection rate greater than 99% when tested with DCMD using seawater. In another work, Kang et al. [18] studied the solvent effects on the membrane hydrophobicity by demonstrating electrospun polystyrene (PS) in various solvents including tetrahydrofuran (THF), chloroform and *N,N*-dimethylformamide (DMF). Electrospun PS/THF (WCA: 138.1°) saw a porous surface morphology whereas PS/CHCl₃ (WCA: 138.8°) had large-scale grooves on individual fibers. The PS/DMF electrospun fibers, showing the most remarkable result among them all (WCA: 154.2°) exhibited protuberant on individual fibers.

Addition of external additives is yet another influential factor towards surface roughness and morphology of resultant fibers. Dong et al. [81] and Ren et al. [88] blended PTFE-PVDF and PDMS-PMMA respectively to fabricate nanofibrous scaffolds by electrospinning. The former produced a treated surface with WCA of 152.2° while the latter achieved 163°. Both treated membranes had salt rejection of 99.99% in MD desalination application. Though the modification basis was similar, PTFE and PMMA, as additives, carried different functions. PTFE lowered the surface energy and enhanced the roughness of membrane whereas PMMA as a carrier mitigated insufficient chain entanglements issue existed in pure PDMS polymer. In another work, Park et al. [89] also presented fabrication of solvent-resistant and mechanically robust electrospinning PVDF nanofibrous network in the presence of tetraethyl orthosilicate (TEOS). The electrospun nanofibrous network yield a WCA of 156°.

A common drawback of electrospun membrane is the inadequacy of mechanical integrity. To address this matter, Zhan et al. [90] demonstrated an advanced electrospinning method. Bead-on-string fibers and micro-sized fibers, both from PS solution were combined homogeneously to manufacture an electrospun sheet by multinozzle electrospinning. The generated electrospun film was rendered superhydrophobic (WCA>150°) with improved mechanical property through combined effect of the two fiber types. Besides, a research work focused on fabricating a superhydrophobic electrospun membrane with blended polyamide 6 (PA6) and PS using a four-jet electrospinning setup [91]. The optimized fibrous mat formed using two PS and two PA6 jets exhibited WCA of 154° and three times increment in tensile strength when compared to the pure PS membrane. Furthermore, coaxial electrospinning, a technique enabling formation of fibers with absence of supporting substrate and reduced usage of hydrophobic material also allowed the manufacturing of core-sheath superhydrophobic AF-PVDF nanofiber membrane with WCA beyond 150° [92].

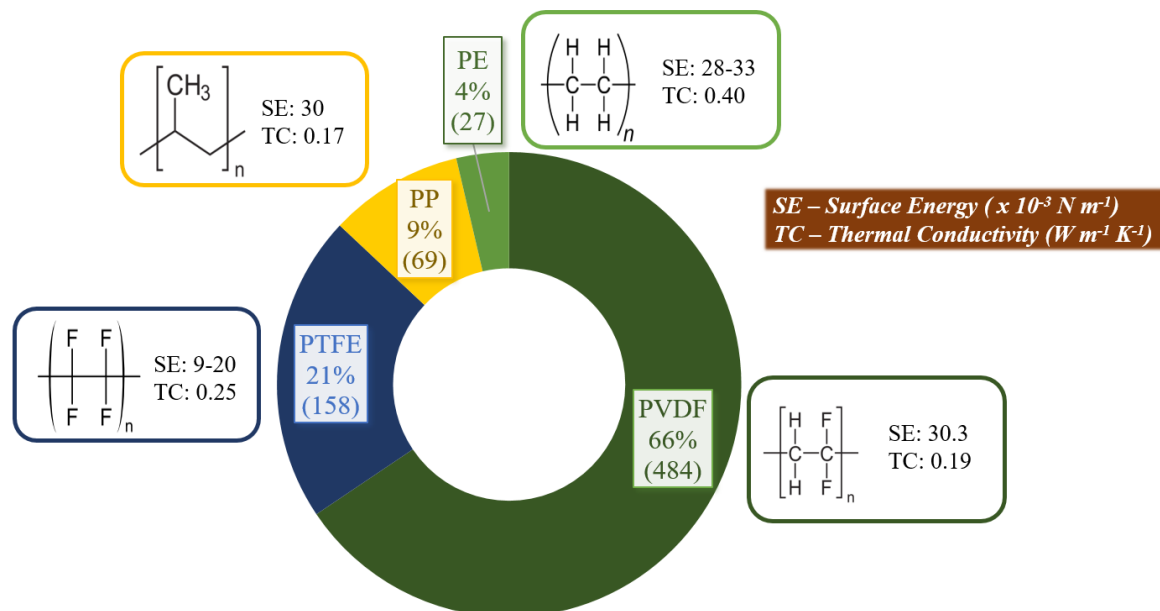


Fig. 4. Percentage distribution (Number of studies) of researches from Scopus of common based materials of polymeric hydrophobic membranes and their properties.

Table 4
Properties of nanoparticles for superhydrophobic modification.

| NPs | CA (°) | NPs Properties | References |
|--------------------------------|-----------|--|------------|
| Al ₂ O ₃ | 154 | Outstanding thermochemical properties, cost effective, low toxicity, handy chemical surface functionalization, high thermal conductivity | [95] |
| SiO ₂ | 150-162.6 | Mild reactivity, good compatibility with organic solvents of polymer dope. It contained high interface adhesive forces with the polymer matrix | [84,96-99] |
| Cera flava | 162 | A solid lipid with low surface energy, consists various hydrophobic components in nature, low cost and easily available | [65] |
| TiO ₂ | 149 | Stable, non-toxic, low cost, anti-fouling | [100] |
| Graphene | 162 | High electrical conductivity with thermal stability, high mechanical stiffness, low water permeability, low cost, good interaction with host polymer, anti-fouling | [41] |

3.2.2. Nanoparticles

Polymer dope solutions containing hydrophobic nanoparticles (NPs) are usually used for fabrication or surface coating to improve membrane's surface roughness [93,94]. Examples of researches using NPs to improve WCA of membranes are summarized in Table 4. For instance, Attia et al. [95] enhanced hydrophobicity of an electrospun PVDF membrane by electrospaying a mixture of non-fluorinated alumina NPs and low concentration of PVDF polymer onto the membrane. By optimizing NPs concentration and volume of dope solution sprayed on the membrane, hierarchical structure was formed on the membrane surface, leading to boosted CA of 154° and LEP of 25 psi.

Indeed, SiO₂ is the most popularly used NPs. For example, hybrid electrospun PVDF-co-hexafluoropropylene (PVDF-HFP)/silica (Si) NPs membrane was synthesised by Hou et al. [84]. The membrane surface was endowed with roughness, attributed to crisscrossing nanofibers and existence of beads-on-string induced by SiNPs incorporation. The addition of NP reduced porosity of membrane, while enlarging pore diameter and thickening the membrane. A good permeate flux and salt rejection of 49 kg/m² h and 99.99% were attained in 240 h continuous MD desalination application. Similarly, silane-functionalized SiO₂ NPs was embedded in PVDF nanofiber through electrospinning, in a work carried out by Nthunya et al. [97], with the highest WCA achieved at 162.6±1.8°. In another work using SiO₂ NPs, Zhang et al. [96] sprayed a mixture of dope containing polydimethylsiloxane (PDMS) and hydrophobic SiO₂ NPs on a PVDF flat sheet membrane. Though there was a slight sacrifice in water flux, the treated membrane exhibited high salt rejection (>99.99%) compared to the neat membrane. Unlike previous examples of direct blending of SiO₂ NPs into polymer matrix, Zhu et al. [99] first linked polydopamine/polyethylenimine (PDA/PEI) composite onto polyimide nanofibrous to render the membrane surface positively charged, followed by binding of SiO₂ NPs (negatively charged) through electrostatic attraction. A high LEP of 42 kPa, MD water permeate of 31 L/m² h and an almost perfect salt rejection were resulted from the modification.

Besides using SiO₂, there are some other researches that succeed in creating superhydrophobic surfaces through embedding NPs in polymer dope solution such as PVDF-HFP-FTES functionalized TiO₂ [100], PVDF-HFP-graphene [41], PSF-Cera flava [65]. For example, Liao et al. [98] carried out integral (I-PVDF) and surface (S-PVDF) modification of electrospun PVDF membrane using silver NPs. While both treated membranes achieved superhydrophobicity, the integrally-modified membrane presented water permeation stabled at around 32 L/m² h when using 3.5 wt.% of NaCl as feed solution in MD operated for 8 h. In contrast, S-PVDF showed significantly unsatisfactory MD flux performance in comparison. This is due to the presence of a dense layer on S-PVDF surface while the silver nanoparticle wrapped around nanofibers had no notable impact on the membrane pores. Furthermore, a WCA of 156.5° was achieved by electrospun conductive and magnetic Fe₃O₄-filled carbon nanofibers. Synergistic effect of superhydrophobic surface with magnetic and conductive properties of carbon nanofibers provide corrosive protection and prevent water intrusion into nanostructures of the carbon fibers [101].

3.2.3. Induced surface roughening upon membrane fabrication

By far, most of the methods to fabricate superhydrophobic membrane involved complicated fabrication procedures or addition of extrinsic additives, thus limiting their practicability in vast applications [19]. Moreover, attrition of the coated additive is probable after long term operations. Many of the low surface energy coated layer are usually non-biodegradable, expensive and have adverse effect towards environment and human health [102]. To induce

surface roughening of membrane directly during the fabrication it can be a solution towards those complex approaches. This technique allows simple construction of appropriate surface roughness without the need of extra hydrophobic additive.

Considering the practicability of membrane manufactured in an industrial scale, different membrane morphology can be fabricated using alcohols (methanol, ethanol) and water as non-solvent [75]. Membrane casted using alcohols has no selective top layer and showed resembled morphology of sponge-like interconnected fibrous structure running through the membrane. On the contrary, presence of an asymmetric dense top layer was reported when water was used as the non-solvent. Roughness of non-solvent methanol fabricated membrane was higher than that of water induced PVDF membrane, giving rise to a promising WCA of 164° and salt rejection greater than 99.99% when tested on DCMD for desalination.

Zhao et al. [19] ventured into nano-casting approach with stainless steel mesh (SSM) and polydimethylsiloxane (PDMS) as the template to fabricate PVDF membrane using phase inversion method. Asymmetric membrane structure was formed, induced by liquid-liquid demixing during the instantaneous phase inversion. Subordinate nano-scale pores were observed in micron-scale topography of the resultant morphology obtained in both PDMS- and SSM-based membranes. The PDMS membrane depicted a knitted surface structure while the SSM-based membrane demonstrated wavy patterns with repeated textures of spike and valley. WCA of both substrate-based membranes was dramatically enhanced (PDMS: 153°, SSM: 164°) but their sliding angles (SA) were of extreme contradiction. PDMS-based membrane, depicting 'petal effect' had SA>90° whereas SSM-based membrane had low SA of 6.8°, agreeing the 'lotus effect'. In addition, DCMD flux increased without compromising salt rejection capacity (>99.99%) in both membranes casted on PDMS and SSM substrates attributed to the enlarged pore size and increased specific surface areas.

3.3. Superhydrophobic membrane enhancement through chemical modifications

Fabrication of membranes using hydrophobic material alone is insufficient to promote anti-wetting behaviour of a membrane to a superhydrophobic level. A fabricated hydrophobic membrane often followed by superhydrophobic modifications which involve roughening of membrane surface as well as lowering of surface energy.

3.3.1. Plasma treatment

Plasma treatment enjoys the benefit of enabling modification of membrane surface without affecting the bulk properties. Depends on the type of gas used, membrane surface can be modified through plasma polymerization, surface reactions or physical etching. Owing to the anisotropic etching of surface layers, plasma treatment can significantly alter micro/nanostructure of the treated surface. For membrane surface superhydrophobic enhancement, fluorine-containing plasma are mostly applied as fluoride species has low surface energy and the C-F bond can be easily activated in plasma [103-105].

For example, CF₄ plasma treatment on PVDF membrane with an IoN 40 plasma system has been carried out at different treatment time by Yang et al. [15] Attributed to low surface tension of fluorinated materials, membrane treated with CF₄ plasma showed improved water contact angles from 130.2±1.11° to 162.4±1.21° at treatment time of 15 min, at which WCA remained nearly constant thereafter. From 15 min onwards, fluorination was deemed reaching saturation. DCMD performance depicted similar trend, whereby a 30% of maximum flux enhancement with salt rejection greater

than 99.98% were observed at 15 min of CF_4 plasma treatment. This was due to the penetration of fluoride gaseous into membrane pores that altered interior structure of membrane and enlarged membrane pores, hence reducing mass transfer resistance. Study by Lin et al. [106] agrees the findings, whereby WCA of treated PP hollow fiber membrane reached plateau (143°) after a 5 min plasma treatment at a working power of 20 W. It is probable that C-F bond formation and breakage reached equilibrium after that time. On top of that, excessive working power was not encouraged as it charred the membrane surface.

In another work, process gas CF_4 was used by Puppolo et al. [107] for hydrophobic treatments of polyethersulfone (PES) and nylon membranes. The treatment engendered both membranes hydrophobic, with WCA of 125° and 135° respectively, a tremendous increment from their untreated superhydrophilic state ($\text{CA } 0^\circ$). Besides, Youngblood et al. [108] controlled PP surface roughness by varying plasma etching time. Highly hydrophobic surfaces were fabricated via PP etching and PTFE sputtering through the technique of inductively coupled radio frequency argon plasma. Similar modification materials and procedure were investigated by Franco et al. [109]. Apart from improving WCA of treated surface by 26° , negligible resistance to mass transfer due to unaltered pore characteristics and thickness as of the neat PP membrane was a merit observed post plasma treatment. Furthermore, the modified structure was able to withstand monoethanolamine (MEA) exposure for a duration of 25 days.

Though fluorinated hydrocarbon is popular in plasma treatment, the highly toxic and corrosive fluorine ions and radicals produced during the plasma process negated its benefits. Hence, non-fluorinated hydrocarbon source is preferable. Lee et al. [105] presented plasma deposition using non-fluorinated hydrocarbon gases included the aromatic benzene, linear aliphatic n-hexane and cyclic aliphatic cyclohexane at ambient conditions. It was reported that deposited aliphatic hydrocarbons could not produce roughen surfaces while benzene was capable of doing so. The film treated with benzene consisted fine nanoparticles, contributing to CA as high as 160° , and the deposition layer remained stably attached to the substrate when immersed in water.

3.3.2. Solvent exchange

Resembling phase inversion method, solvent exchange technique induced re-conformation of polymer on membrane surfaces, leading to desired surface roughness. Addition of non-solvent in homogeneous polymer-solvent solution causes aggregation of micro- and nano-scaled papillae when solvent evaporated [103]. Utilizing Methyl-ethyl ketone (MEK) as the non-solvent and PP as the coating polymer, PP membrane has been successfully modified to achieve a static CA of $169 \pm 1^\circ$, a 42° improvement as compared to the untreated PP membrane [110]. Surface roughness of the chemically treated PP membrane was immensely enhanced with concentration of PP in solution and coating drying temperature optimized at 17.9 mg/ml and 70°C , respectively.

Ji et al. [111] replicated this method with acetone acted as the precipitator that promoted crystallization of PP polymer on the treated surface. A stable superhydrophobic surface (tested with aqueous solution of pH ranged from 2 to 12) and WCA as high as $160 \pm 1.9^\circ$ was achieved. Similarly, Lv et al. [112] spin coated PP hollow fibre membrane with mixture of PP solution containing both cyclohexanone and MEK. At non-solvent ratio of 1:1, a good homogeneity and crystallites distribution resulted in a treated surface with WCA of 158° . Effect of film formation temperature, polymer concentration and the non-solvent on homogeneity, surface roughness and WCA of isotactic polypropylene (*i*-PP) coating had also been studied by Erbil et al. [113]. Mixing of non-solvent was found to improve coating homogeneity, rendering reduced size of *i*-PP crystallites and narrower cylindrical bridges with wider pores distribution, which led to dramatic enhancement of WCA. In another work, an astonished LDPE coated surface with WCA of $173 \pm 2.5^\circ$ was fabricated through adjusting nucleation rate and crystallization time. In the study, cyclohexanone was used as the non-solvent [114]. Florallike crystal structures, which responsible for the superhydrophobicity were formed after the chemical treatment.

PVC solution and non-solvent ethanol, water and acetone were adopted to render a surface with WCA of $155.3 \pm 1.9^\circ$ in a study conducted by Li et al. [115]. When non-solvent interacts with solvent, surface tension shrank, hence breaking interface between them, which then caused micro-phase separation of PVC solution. Solidification took place soon after, subsequently forming micro- or nano-papillae. Instead of mixing non-solvent in solvent, Himma et al. [16] performed a two steps dip coating whereby the PP membrane was first coated with MEK (non-solvent), followed immediately by PP solution. This method is advantageous over the aforementioned technique as it left PP solubility in the solution undisrupted thus preventing PP crystallization in solution before coating on targeted surface.

Effort was devoted by Qing et al. [102] to manipulate both surface

chemistry and the surface roughness of PVDF electrospun membrane via a one-step solvent-thermal induced roughening (STIR) process. Alcohols of different chain-length were used as the treatment solvent. During the treatment, soft-shell of nanofibers swelled whereas the inner hard-core remained intact, causing shell deformation due to mismatched internal stress between shell and core. The deformation subsequently led to formation of nanofin structure on the nanofibers hence promoted surface roughness. Meanwhile, different alcohols also responsible for tuning PVDF nanofiber surface chemistry by controlling the fraction distribution of crystal phases. The phases include nonpolar α phase (responsible for low surface energy) and polar β phase. 1-pentanol, an alcohol of moderate affinity, appeared to be the most optimized alcohol preference, as it resulted in the highest surface roughness. Thus, led to the best anti wetting ability (WCA: 164.1°), promoted increased density of α phase and the highest DCMD permeate at $21 \text{ kg/m}^2\text{h}$ when tested with NaCl of 3.5 wt. % as feed.

3.3.3. Sol-gel

A sol is usually prepared through a network formation process that involves hydrolysis and polycondensation of the corresponding oxide. A large amount of solvent is impregnated in the network during the process, thus forming a gel. The sol-gel method possess great opportunities to impose superhydrophobic characteristics on modified membranes as composition of reaction mixtures and membrane surface roughness can be handily tuned by altering the method protocol [104]. It is also worth mentioning that superhydrophobic modification through sol-gel method provides a stable and robust coating due to covalent bonds formation between the coating dope and substrate by condensation during the sol-gel process or/and dehydration in the curing process [116]. In a work carried out by Sun et al. [17], a hydrophilic PES surface was transformed into superhydrophobic (WCA: 154°) state via sol-gel process that harnessed NH_4OH as catalyst, TEOS as precursor and ethanol as solvent. Dodecafluorooctylpropyl-trimethoxysilane (DPT-12) was made used for fluorination after the gel formation to further lower the surface energy. Embracing similar materials and technique, Li et al. [117] reported that heterogeneity and fluorinated groups presence on membrane surface were responsible for membrane hydrophobicity. WCA of membrane with optimized treatment conditions was 156° . Unfortunately, excessive fluorination led to deterioration of surface roughness. In another work, Raveshiyani et al. [118] treated *i*-PP membrane with Piranha to increase OH group density on the membrane surface, followed by coating of perfluorooctyltriethoxysilane (PFOTES) and TEOS mixture. It was found that the fluorinated silica nanoparticles exist on the surface as well as in the cross section of the porous membrane, creating a superhydrophobic surface with WCA of 168° .

Study of the synergy effects of nanofillers and sol-gel technique was carried out by Meng et al. [119], where TiO_2 was used as the sol-gel templating agent. After sol-gel process, 1H,1H,2H,2H-perfluorododecyltrichlorosilane (FTCS) was then filtered through the modified PVDF membrane, making it superhydrophobic with WCA greater than 150° . Similar work was also found by incorporating perfluoroalkylmethacrylic copolymerin, a composite sol-gel matrix contained of fumed silica nanoparticles [120]. From the study, the membrane produced a surface WCA of 158° . Besides, a single-step approach to synthesize self-cleaning surface through sol-gel technique of long-chain fluoroalkylsilane has been reported by Liu et al. [121]. The coating surface with WCA of 169° depicted a wrinkled, rough, and hill-like morphology with promising stability and durability.

4. Future prospects and directions of MD

As MD has the ability to treat wastewater containing phosphorus, nitrogenous wastes, and high salt content, one can venture into its potentials to treat effluent from aquaculture farms as future research directions. Since late 1980s, global capture fishery production is relatively static, indicating the catch fishery has been exploited to its limit. Aquaculture, a profitable aquatic species cultivation activity hence emerged as an imperative initiative to bridge the supply and demand gap of aquatic products [122-124]. Albeit aquaculture stands as the most rapidly growing food production sector in the world, further grow surge is still anticipated to cope with the world's demand in which an estimation of 62% of food fish is in need from aquaculture production by year 2030 [125]. Though aquaculture succeeds in paving future needs of food, its development paradoxically associates with paramount of criticisms, particularly on sustainability, environment and social degrading issues. Some examples include wetlands and mangrove forests destruction [126], undesired freshwater salinization [127], and bio-accumulation of antibiotics and drugs used to control fish diseases [124]. In general,

wastewater from aquaculture is usually saline [128] and rich in complex compounds, such as ammonia (NH_3), nitrate (NO_3^-), nitrite (NO_2^-), phosphorus (P) and total suspended solid (TSS) [129,130]. A number of publications related to amount of constituents in aquaculture water are listed in Table 5. Besides, a minor portion of the waste constituent is contributed by bacteria and pathogens from the concentrated feed operation [131,132]. Degradation of other bodies of water by aquaculture wastewater is always a concern. For example, ammonia and nitrite are deemed toxic and the presence of nitrate stimulates hypertrophication [129]. This phenomenon potentially leads to huge fish kills, shellfish contamination and worse, to induce latent health hazard to humans [133].

Other than available conventional aquaculture wastewater treatment technologies, a number of membrane based technologies emerged to be effective to treat effluent from aquaculture. A wind driven RO with applied pressure of 4.83 to 7.58 bar was capable to remove 90 to 97% nitrogen from aquaculture effluent at flux of 228 to 366 L/h depends on wind speed [139]. Besides, at fluxes of 0.499 to 0.712 L/m² h, retentions of 85% total ammonia and 95% phosphorus from aquaculture wastewater were attained by a dead end permeation cell using polysulfone nanofiltration membrane with applied pressure of 6 to 10 bar [133]. Also deploying dead end permeation cell, but using polyethersulfone membrane, Nora'aini et al.'s [140] work successfully removed 96% total phosphorus and 86% ammonium from effluent of aquaculture at fluxes of 17.39 to 27.9 L/m² h.

Apart from complex compounds, as mentioned earlier, aquaculture wastewater comprises of high salt content, be it offshore [141-143] or land [128,144-146] based aquaculture farms as salts are mainly used to reduce fish stress [130]. In a review written by Castine et al. [128], it was found that salinities of marine and brackish water land-based aquaculture systems of shrimp industry in Australia are 30-50‰ and 0.5-30‰ respectively. A study by Hickman et al. [145] induced that growth rate of *Colistium nudipinnis* was affected by the salinity (33-18 g/L) of the aquaculture water. Moving on, the Kasetsart University Khlongwan fishery research station in Thailand recorded salinities ranged between 0.1-3.2‰ [146]. Another research that studied

survivability of juvenile cobia out of its original oceanic environment (salinity ~34 ppt) indicated that juvenile cobia was able to survive at salinity as low as 5 ppt, provided highly bioavailable source of minerals were supplied to the culture feed [144].

Currently, there is no study about employing MD to treat aquaculture wastewater. Yet, as discussed thoroughly in the review, MD is capable to treat high salinity water, as well as complex compounds found in aquaculture water (Table 5). In fact, the flux and rejection performances of MD in separating salt, nitrogenous waste and phosphorus from wastewater as mentioned in section 2.0 outperform the aforementioned membrane technologies. As such, MD is a highly prospective separation application to be ventured into to treat aquaculture wastewater. Additionally, paramount of efforts are still needed to evaluate and refine associated parameters towards mature implementation of MD to treat aquaculture wastewater. Some crucial considerations include robustness of the process and possibility of large scale production of the MD membrane. Availability, price and environmental impact of raw materials for manufacturing and modification of MD membrane should also be taken into consideration.

Besides exhibiting laudable possibilities in treating effluent from aquaculture, MD sees other rooms of amelioration for its operations and applications, in terms of enhancement of its operational efficiency and sustainability. Other than aforementioned membrane modification techniques, blending of membrane fabrication polymers and/or superhydrophobic treatment, which expect to compliment shortages of their counterparts can be further investigated. Since MD has the ability to operate at high salt concentration, one should venture into hybrid of MD with other desalination technologies such as reverse osmosis, forward osmosis, crystallization and bioreactor to boost overall performance [10]. Restoration of membrane workability after wetting is another worth studying matter. To date, the only strategy that proves to succeed in recovering liquid-vapour interface at the membrane pores is to increase the feed temperature [66]. More initiative should be imposed in this area to prolong MD's usability.

Table 5
Constituent of complex compounds in aquaculture water.

| Habitat | Species | Aquaculture Water Constituent (mg/L) | | | | | pH | Ref. |
|-----------------------------------|--------------------|--------------------------------------|-----------------|-----------------|-----------|------------|-----|-------|
| | | NH_3 | NO_3^- | NO_2^- | P | TSS | | |
| Haraz river, Iran | Vana rainbow trout | - | 1.88 | 0.024 | 0.25 | 16.06 | 8.4 | [134] |
| Land based aquaculture, Australia | Shrimp | 0.41 | 0.091-0.19 | 0.004-0.23 | 0.02-0.28 | 0.40-76.80 | - | [128] |
| Alabama, United States | Channel Catfish | 1.09 | - | - | 0.25 | 70.00 | 8.2 | [135] |
| SDC Farm, Nigeria | Catfish | 1.17 | 9.93 | - | 18.43 | 2136.75 | 6.8 | [136] |
| Nebraska, United States | Trout | 0.02 | - | - | 0.17 | 10.00 | - | [137] |
| Wisconsin, United States | Perch | 0.20 | - | - | 0.04 | 7.50 | - | [137] |
| Iowa, United States | Catfish | 0.15 | - | - | 0.15 | 12.00 | - | [137] |
| Parana, Brazil | Tilapia | 1.52 | 0.70 | 0.23 | 1.88 | 244.25 | 6.6 | [138] |

5. Conclusion

The surging demand on purifying saline water has bolstered thriving growth of desalination technologies. The prosperous development of conventional desalination techniques, including RO and MSF, however suffered from limitations on energy efficiencies, feed salt concentrations and serious membrane clogging issues. MD process, a thermally driven separation process is therefore introduced as a potential high salinity wastewater treatment process to constructively address the concerns mentioned above. Though MD process is capable to treat saline wastewaters of various constituents and varied salt concentrations, challenges such as membrane pore wetting and fouling on the other hand, impede smooth development of MD process. Wetting mechanism, as well as solutions towards challenges of MD membranes were comprehensively detailed in this review. To maximize and retain MD's functionality, MD membranes were fabricated using hydrophobic materials, followed by superhydrophobic enhancements which involved a huge diversity of techniques. In future, MD can be adopted to treat aquaculture wastewater, while hybridization of MD with other desalination systems and restoration of membrane's effective mass transfer surface possess possibilities to further boost up its operational efficiencies.

Acknowledgement

This work is supported by MOHE Transdisciplinary Research Grant Scheme (TRGS/1/2018/USM/01/5/1; Account No. TRGS/203/PJKIMIA/67612001). Chin Jing Yi acknowledges academic financial support awarded by Universiti Sains Malaysia Fellowship Scheme.

References

- [1] R. Ullah, M. Khraisheh, R. J. Esteves, J. T. McLeskey Jr, M. AlGhouthi, M. Gad-el-Hak, H. V. Tafreshi, Energy efficiency of direct contact membrane distillation, *Desalination*. 433 (2018) 56-67. <https://doi.org/10.1016/j.desal.2018.01.025>
- [2] L.-F. Ren, F. Xia, V. Chen, J. Shao, R. Chen, Y. He, TiO₂-FTCS modified superhydrophobic PVDF electrospun nanofibrous membrane for desalination by direct contact membrane distillation, *Desalination*. 423 (2017) 1-11. <https://doi.org/10.1016/j.desal.2017.09.004>
- [3] C. Li, X. Li, L. Qin, W. Wu, Q. Meng, C. Shen, G. Zhang, Membrane photobioreactor coupled with heterogeneous Fenton fluidized bed for high salinity wastewater treatment: Pollutant removal, photosynthetic bacteria harvest and membrane anti-fouling analysis, *Sci. Tot. Environ.* 696 (2019) 133953.

- <https://doi.org/10.1016/j.scitotenv.2019.133953>
- [4] Y. W. Berkessa, Q. Lang, B. Yan, S. Kuang, D. Mao, L. Shu, Y. Zhang, Anion exchange membrane organic fouling and mitigation in salt valorization process from high salinity textile wastewater by bipolar membrane electro dialysis, *Desalination*. 465 (2019) 94–103. <https://doi.org/10.1016/j.desal.2019.04.027>
- [5] H. Cho, Y. Choi, S. Lee, J. Sohn, J. Koo, Membrane distillation of high salinity wastewater from shale gas extraction: effect of antiscalants, *Desalin. Water Treat.* 57 (2016) 26718–26729. <https://doi.org/10.1080/19443994.2016.1190109>
- [6] Y. Magara, M. Kawasaki, M. Sekino, H. Yamamura, Development of reverse osmosis membrane seawater desalination in Japan, *Water Sci. Technol.* 41 (2000) 1–8. <https://doi.org/10.2166/wst.2000.0594>
- [7] S. M. A. Moustafa, D. I. Jarrar, H. I. El-Mansy, Performance of a self-regulating solar multistage flash desalination system, *Solar Energy*. 35 (1985) 333–340. [https://doi.org/10.1016/0038-092X\(85\)90141-0](https://doi.org/10.1016/0038-092X(85)90141-0)
- [8] E. K. Summers, H. A. Arafat, Energy efficiency comparison of single-stage membrane distillation (MD) desalination cycles in different configurations, *Desalination*. 290 (2012) 54–66. <https://doi.org/10.1016/j.desal.2012.01.004>
- [9] P. Biniiaz, N. Torabi Ardekani, M. A. Makarem, M. R. Rahimpour, Water and Wastewater Treatment Systems by Novel Integrated Membrane Distillation (MD), *Chem. Eng.* 3 (2019) 8. <https://doi.org/10.3390/chemengineering3010008>
- [10] P. Wang, T.-S. Chung, Recent advances in membrane distillation processes: Membrane development, configuration design and application exploring, *J. Membr. Sci.* 474 (2015) 39–56. <https://doi.org/10.1016/j.memsci.2014.09.016>
- [11] S. Al-Obaidani, E. Curcio, F. Macedonio, G. Di Profio, H. Al-Hinai, E. Drioli, Potential of membrane distillation in seawater desalination: Thermal efficiency, sensitivity study and cost estimation, *J. Membr. Sci.* 323 (2008) 85–98. <https://doi.org/10.1016/j.memsci.2008.06.006>
- [12] Y. Zhang, Y. Peng, S. Ji, Z. Li, P. Chen, Review of thermal efficiency and heat recycling in membrane distillation processes, *Desalination*. 367 (2015) 223–239. <https://doi.org/10.1016/j.desal.2015.04.013>
- [13] H. Fan, Y. Peng, Application of PVDF membranes in desalination and comparison of the VMD and DCMD processes, *Chem. Eng. Sci.* 79 (2012) 94–102. <https://doi.org/10.1016/j.ces.2012.05.052>
- [14] H. C. Duong, P. Cooper, B. Nelemans, T. Y. Cath, L. D. Nghiem, Optimising thermal efficiency of direct contact membrane distillation by brine recycling for small-scale seawater desalination, *Desalination*. 374 (2015) 1–9. <https://doi.org/10.1016/j.desal.2015.07.009>
- [15] C. Yang, X.-M. Li, J. Gilron, D.-f. Kong, Y. Yin, Y. Oren, C. Linder, T. He, CF4 plasma-modified superhydrophobic PVDF membranes for direct contact membrane distillation, *J. Membr. Sci.* 456 (2014) 155–161. <https://doi.org/10.1016/j.memsci.2014.01.013>
- [16] N. F. Himma, A. K. Wardani, I. G. Wenten, Preparation of superhydrophobic polypropylene membrane using dip-coating method: the effects of solution and process parameters, *Polym. Plast. Technol. Eng.* 56 (2017) 184–194. <https://doi.org/10.1080/03602559.2016.1185666>
- [17] X. Sun, Effects of the Based Membrane on the Hydrophobicity of Superhydrophobic PES Membrane and its Structural Properties, *Mod. Appl. Sci.* 4 (2010) 71. <https://doi.org/10.5539/mas.v4n2p71>
- [18] M. Kang, R. Jung, H.-S. Kim, H.-J. Jin, Preparation of superhydrophobic polystyrene membranes by electrospinning, *Colloids Surf. A Physicochem. Eng. Asp.* 313 (2008) 411–414. <https://doi.org/10.1016/j.colsurfa.2007.04.122>
- [19] F. Zhao, Z. Ma, K. Xiao, C. Xiang, H. Wang, X. Huang, S. Liang, Hierarchically textured superhydrophobic polyvinylidene fluoride membrane fabricated via nanocasting for enhanced membrane distillation performance, *Desalination*. 443 (2018) 228–236. <https://doi.org/10.1016/j.desal.2018.06.003>
- [20] X. Zhang, F. Shi, J. Niu, Y. Jiang, Z. Wang, Superhydrophobic surfaces: from structural control to functional application, *J. Mater. Chem.* 18 (2008) 621–633. <https://doi.org/10.1039/B711226B>
- [21] G. H. Teoh, J. Y. Chin, B. S. Ooi, Z. A. Jawad, H. T. L. Leow, S. C. Low, Superhydrophobic membrane with hierarchically 3D-microtexture to treat saline water by deploying membrane distillation, *J. Water Process. Eng.* 37 (2020) 101528. <https://doi.org/10.1016/j.jwpe.2020.101528>
- [22] N. A. Azmi, S. H. Ahmad, S. C. Low, Detection of mercury ions in water using a membrane-based colorimetric sensor, *RSC Adv.* 8 (2018) 251–261. <https://doi.org/10.1039/C7RA11450H>
- [23] H. P. Ngang, A. L. Ahmad, S. C. Low, B. S. Ooi, Adsorption-desorption study of oil emulsion towards thermo-responsive PVDF/SiO₂-PNIPAM composite membrane, *J. Environ. Chem. Eng.* 5 (2017) 4471–4482. <https://doi.org/10.1016/j.jece.2017.08.038>
- [24] R. Shaimi, S. C. Low, Morphological characteristics of polymeric nylon-6 film as biological recognition interface for electrochemical immunosensor application, *J. Appl. Polym. Sci.* 135 (2018) 46741. <https://doi.org/10.1002/app.46741>
- [25] Y. Chen, M. Tian, X. Li, Y. Wang, A. K. An, J. Fang, T. He, Anti-wetting behavior of negatively charged superhydrophobic PVDF membranes in direct contact membrane distillation of emulsified wastewaters, *J. Membr. Sci.* 535 (2017) 230–238. <https://doi.org/10.1016/j.memsci.2017.04.040>
- [26] T. Vazirnejad, J. Karimi-Sabet, A. Dastbaz, M. A. Moosavian, S. A. Ghorbanian, Application of Salt Additives and Response Surface Methodology for Optimization of PVDF Hollow Fiber Membrane in DCMD and AGMD Processes, *J. Membr. Sci. Res.* 2 (2016) 169–178. <https://doi.org/10.22079/jmsr.2016.21947>
- [27] L. M. Camacho, L. Dumée, J. Zhang, J.-d. Li, M. Duke, J. Gomez, S. Gray, Advances in membrane distillation for water desalination and purification applications, *Water*. 5 (2013) 94–196. <https://doi.org/10.3390/w5010094>
- [28] V. Karanikola, S. E. Moore, A. Deshmukh, R. G. Arnold, M. Elimelech, A. E. Sáez, Economic performance of membrane distillation configurations in optimal solar thermal desalination systems, *Desalination*. 472 (2019) 114164. <https://doi.org/10.1016/j.desal.2019.114164>
- [29] H. C. Duong, P. Cooper, B. Nelemans, T. Y. Cath, L. D. Nghiem, Evaluating energy consumption of air gap membrane distillation for seawater desalination at pilot scale level, *Sep. Purif. Technol.* 166 (2016) 55–62. <https://doi.org/10.1016/j.seppur.2016.04.014>
- [30] G. Mannella, V. La Carrubba, V. Brucato, Evaluation of vapor mass transfer in various membrane distillation configurations: an experimental study, *Heat Mass Transf.* 48 (2012) 945–952. <https://doi.org/10.1007/s00231-011-0946-x>
- [31] E. El-Zanati, M. Khedr, A. El-Gendi, H. Abdallah, E. Farg, E. Taha, Heat and mass transfer characteristics in vacuum membrane distillation for water desalination, *Desalin. Water Treat.* 132 (2018) 52–62. <https://doi.org/10.5004/dwt.2018.23032>
- [32] M. R. Shirzad Kebria, A. Rahimpour, Membrane Distillation: Basics, Advances, and Applications, *Adv. Membr. Technol.*, 2020, pp. 1–21.
- [33] S. Kim, D. W. Lee, J. Cho, Application of direct contact membrane distillation process to treat anaerobic digester, *J. Membr. Sci.* 511 (2016) 20–28. <https://doi.org/10.1016/j.memsci.2016.03.038>
- [34] A. Boubakri, A. Hafiane, S. Al Tahar Bouguecha, Nitrate removal from aqueous solution by direct contact membrane distillation using two different commercial membranes, *Desalin. Water Treat.* 56 (2015) 2723–2730. <https://doi.org/10.1080/19443994.2014.981408>
- [35] M. El-Bourawi, M. Khayet, R. Ma, Z. Ding, Z. Li, X. Zhang, Application of vacuum membrane distillation for ammonia removal, *J. Membr. Sci.* 301 (2007) 200–209. <https://doi.org/10.1016/j.memsci.2007.06.021>
- [36] D. Qu, D. Sun, H. Wang, Y. Yun, Experimental study of ammonia removal from water by modified direct contact membrane distillation, *Desalination*. 326 (2013) 135–140. <https://doi.org/10.1016/j.desal.2013.07.021>
- [37] X. Li, M. García-Payo, M. Khayet, M. Wang, X. Wang, Superhydrophobic polysulfone/polydimethylsiloxane electrospun nanofibrous membranes for water desalination by direct contact membrane distillation, *J. Membr. Sci.* 542 (2017) 308–319. <https://doi.org/10.1016/j.memsci.2017.08.011>
- [38] Q. Su, J. Zhang, L.-Z. Zhang, Fouling resistance improvement with a new superhydrophobic electrospun PVDF membrane for seawater desalination, *Desalination*. 476 (2020) 114246. <https://doi.org/10.1016/j.desal.2019.114246>
- [39] M. H. Abd Aziz, M. H. Dzarfan Othman, N. H. Alias, T. Nakayama, Y. Shingaya, N. A. Hashim, T. A. Kurniawan, T. Matsuura, M. A. Rahman, J. Jaafar, Enhanced omniphobicity of multilayer hollow fiber membrane with organosilane-functionalized TiO₂ micro-flowers and nanorods layer deposition for desalination using direct contact membrane distillation, *J. Membr. Sci.* 607 (2020) 118137. <https://doi.org/10.1016/j.memsci.2020.118137>
- [40] Y.-X. Huang, Z. Wang, J. Jin, S. Lin, Novel Janus membrane for membrane distillation with simultaneous fouling and wetting resistance, *Environ. Sci. Technol.* 51 (2017) 13304–13310. <https://doi.org/10.1021/acs.est.7b02848>
- [41] Y. C. Woo, L. D. Tijing, W.-G. Shim, J.-S. Choi, S.-H. Kim, T. He, E. Drioli, H. K. Shon, Water desalination using graphene-enhanced electrospun nanofiber membrane via air gap membrane distillation, *J. Membr. Sci.* 520 (2016) 99–110. <https://doi.org/10.1016/j.memsci.2016.07.049>
- [42] L. García-Fernández, B. Wang, M. C. García-Payo, K. Li, M. Khayet, Morphological design of alumina hollow fiber membranes for desalination by air gap membrane distillation, *Desalination*. 420 (2017) 226–240. <https://doi.org/10.1016/j.desal.2017.07.021>
- [43] S. Cemeaux, I. Strużyńska, W. M. Kujawski, M. Persin, A. Larbot, Comparison of various membrane distillation methods for desalination using hydrophobic ceramic membranes, *J. Membr. Sci.* 337 (2009) 55–60. <https://doi.org/10.1016/j.memsci.2009.03.025>
- [44] L. Li, J.-W. Wang, H. Zhong, L.-Y. Hao, H. Abadikhah, X. Xu, C.-S. Chen, S. Agathopoulos, Novel α -Si₃N₄ planar nanowire superhydrophobic membrane prepared through in-situ nitridation of silicon for membrane distillation, *J. Membr. Sci.* 543 (2017) 98–105. <https://doi.org/10.1016/j.memsci.2017.08.049>
- [45] S. Tao, Y.-D. Xu, J.-Q. Gu, H. Abadikhah, J.-W. Wang, X. Xu, Preparation of high-efficiency ceramic planar membrane and its application for water desalination, *J. Adv. Ceram.* 7 (2018) 117–123. <https://doi.org/10.1007/s40145-018-0263-7>
- [46] A. Alhathal Alanezi, H. Abdallah, E. El-Zanati, A. Ahmad, A. O. Sharif, Performance investigation of O-ring vacuum membrane distillation module for water desalination, *J. Chem.* 2016 (2016) 2016. <https://doi.org/10.1155/2016/9378460>
- [47] C. Hu, Z. Yang, Q. Sun, Z. Ni, G. Yan, Z. Wang, Facile Preparation of a Superhydrophobic iPP Microporous Membrane with Micron-Submicron Hierarchical Structures for Membrane Distillation, *Polymers*. 12 (2020) 2009. <https://doi.org/10.3390/polym12040092>
- [48] J. E. Efome, M. Baghbanzadeh, D. Rana, T. Matsuura, C. Q. Lan, Effects of superhydrophobic SiO₂ nanoparticles on the performance of PVDF flat sheet membranes for vacuum membrane distillation, *Desalination*. 373 (2015) 47–57. <https://doi.org/10.1016/j.desal.2015.07.002>
- [49] K.-K. Yan, L. Jiao, S. Lin, X. Ji, Y. Lu, L. Zhang, Superhydrophobic electrospun nanofiber membrane coated by carbon nanotubes network for membrane distillation, *Desalination*. 437 (2018) 26–33. <https://doi.org/10.1016/j.desal.2018.02.020>
- [50] X. Chen, X. Gao, K. Fu, M. Qiu, F. Xiong, D. Ding, Z. Cui, Z. Wang, Y. Fan, E. Drioli, Tubular hydrophobic ceramic membrane with asymmetric structure for water

- desalination via vacuum membrane distillation process, *Desalination*, 443 (2018) 212–220. <https://doi.org/10.1016/j.desal.2018.05.027>
- [51] J. Kim, K. Park, D. R. Yang, S. Hong, A comprehensive review of energy consumption of seawater reverse osmosis desalination plants, *Appl. Energy*, 254 (2019) 113652. <https://doi.org/10.1016/j.apenergy.2019.113652>
- [52] B. Li, K. K. Sirkar, Novel membrane and device for vacuum membrane distillation-based desalination process, *J. Membr. Sci.* 257 (2005) 60–75. <https://doi.org/10.1016/j.memsci.2004.08.040>
- [53] L. F. Greenlee, D. F. Lawler, B. D. Freeman, B. Marrot, P. Moulin, Reverse osmosis desalination: Water sources, technology, and today's challenges, *Water Res.* 43 (2009) 2317–2348. <https://doi.org/10.1016/j.watres.2009.03.010>
- [54] Y.-D. Kim, K. Thu, N. Ghaffour, K. Choon Ng, Performance investigation of a solar-assisted direct contact membrane distillation system, *J. Membr. Sci.* 427 (2013) 345–364. <https://doi.org/10.1016/j.memsci.2012.10.008>
- [55] F. E. Ahmed, R. Hashaikeh, N. Hilal, Solar powered desalination – Technology, energy and future outlook, *Desalination*, 453 (2019) 54–76. <https://doi.org/10.1016/j.desal.2018.12.002>
- [56] Q. Li, L.-J. Beier, J. Tan, C. Brown, B. Lian, W. Zhong, Y. Wang, C. Ji, P. Dai, T. Li, P. Le Clech, H. Tyagi, X. Liu, G. Leslie, R. A. Taylor, An integrated, solar-driven membrane distillation system for water purification and energy generation, *Appl. Energy*, 237 (2019) 534–548. <https://doi.org/10.1016/j.apenergy.2018.12.069>
- [57] A. Criscuolo, Improvement of the Membrane Distillation performance through the integration of different configurations, *Chem. Eng. Res. Des.* 111 (2016) 316–322. <https://doi.org/10.1016/j.cherd.2016.05.020>
- [58] G. W. Meindersma, C. M. Guijt, A. B. de Haan, Desalination and water recycling by air gap membrane distillation, *Desalination*, 187 (2006) 291–301. <https://doi.org/10.1016/j.desal.2005.04.088>
- [59] Y. M. Manawi, M. Khraisheh, A. K. Fard, F. Benyahia, S. Adham, Effect of operational parameters on distillate flux in direct contact membrane distillation (DCMD): Comparison between experimental and model predicted performance, *Desalination*, 336 (2014) 110–120. <https://doi.org/10.1016/j.desal.2014.01.003>
- [60] O. R. Lokare, R. D. Vidic, Impact of Operating Conditions on Measured and Predicted Concentration Polarization in Membrane Distillation, *Environmental Science & Technology*, 53 (2019) 11869–11876. <https://doi.org/10.1021/acs.est.9b04182>
- [61] Y. Choi, G. Naidu, S. Jeong, S. Vigneswaran, S. Lee, R. Wang, A. G. Fane, Experimental comparison of submerged membrane distillation configurations for concentrated brine treatment, *Desalination*, 420 (2017) 54–62. <https://doi.org/10.1016/j.desal.2017.06.024>
- [62] Z. Wang, Y. Chen, S. Lin, Kinetic model for surfactant-induced pore wetting in membrane distillation, *J. Membr. Sci.* 564 (2018) 275–288. <https://doi.org/10.1016/j.memsci.2018.07.010>
- [63] M. Rezaei, D. M. Warsinger, M. C. Duke, T. Matsuura, W. M. Samhaber, Wetting phenomena in membrane distillation: mechanisms, reversal, and prevention, *Water Res.* 139 (2018) 329–352. <https://doi.org/10.1016/j.watres.2018.03.058>
- [64] S. M. Seyed Shahabadi, H. Rabiee, S. M. Seyedi, A. Mokhtare, J. A. Brant, Superhydrophobic dual layer functionalized titanium dioxide/polyvinylidene fluoride-co-hexafluoropropylene (TiO₂/PH) nanofibrous membrane for high flux membrane distillation, *J. Membr. Sci.* 537 (2017) 140–150. <https://doi.org/10.1016/j.memsci.2017.05.039>
- [65] S. S. Ray, S.-S. Chen, C. T. N. Dan, H.-T. Hsu, H.-M. Chang, N. C. Nguyen, H.-T. Nguyen, Casting of a superhydrophobic membrane composed of polysulfone/Ceraflava for improved desalination using a membrane distillation process, *RSC Adv.* 8 (2018) 1808–1819. <https://doi.org/10.1039/C7RA12474K>
- [66] E. Guillen-Burrieza, M. Mavukkandy, M. Bilad, H. Arafat, Understanding wetting phenomena in membrane distillation and how operational parameters can affect it, *J. Membr. Sci.* 515 (2016) 163–174. <https://doi.org/10.1016/j.memsci.2016.05.051>
- [67] D. M. Warsinger, J. Swaminathan, E. Guillen-Burrieza, H. A. Arafat, Scaling and fouling in membrane distillation for desalination applications: a review, *Desalination*, 356 (2015) 294–313. <https://doi.org/10.1016/j.desal.2014.06.031>
- [68] M. Gryta, Desalination of thermally softened water by membrane distillation process, *Desalination*, 257 (2010) 30–35. <https://doi.org/10.1016/j.desal.2010.03.012>
- [69] X.-Q. Wu, X. Wu, T.-Y. Wang, L. Zhao, Y. B. Truong, D. Ng, Y.-M. Zheng, Z. Xie, Omniphobic surface modification of electrospun nanofiber membrane via vapor deposition for enhanced anti-wetting property in membrane distillation, *J. Membr. Sci.* 606 (2020) 118075. <https://doi.org/10.1016/j.memsci.2020.118075>
- [70] B. J. Deka, J. Guo, N. K. Khanzada, A. K. An, Omniphobic re-entrant PVDF membrane with ZnO nanoparticles composite for desalination of low surface tension oily seawater, *Water Research*, 165 (2019) 114982. <https://doi.org/10.1016/j.watres.2019.114982>
- [71] J. Li, S. Guo, Z. Xu, J. Li, Z. Pan, Z. Du, F. Cheng, Preparation of omniphobic PVDF membranes with silica nanoparticles for treating coking wastewater using direct contact membrane distillation: Electrostatic adsorption vs. chemical bonding, *J. Membr. Sci.* 574 (2019) 349–357. <https://doi.org/10.1016/j.memsci.2018.12.079>
- [72] Y. Chul Woo, Y. Chen, L. D. Tijing, S. Phuntsho, T. He, J.-S. Choi, S.-H. Kim, H. Kyong Shon, CF₄ plasma-modified omniphobic electrospun nanofiber membrane for produced water brine treatment by membrane distillation, *J. Membr. Sci.* 529 (2017) 234–242. <https://doi.org/10.1016/j.memsci.2017.01.063>
- [73] S. Wang, Y. Li, X. Fei, M. Sun, C. Zhang, Y. Li, Q. Yang, X. Hong, Preparation of a durable superhydrophobic membrane by electrospinning poly(vinylidene fluoride) (PVDF) mixed with epoxy-siloxane modified SiO₂ nanoparticles: A possible route to superhydrophobic surfaces with low water sliding angle and high water contact angle, *J. Colloid Interf. Sci.* 359 (2011) 380–388. <https://doi.org/10.1016/j.jcis.2011.04.004>
- [74] X.-M. Li, T. He, M. Crego-Calama, D. N. Reinhoudt, Conversion of a metastable superhydrophobic surface to an ultrahydrophobic surface, *Langmuir*, 24 (2008) 8008–8012. <https://doi.org/10.1021/la801044j>
- [75] S. Munirasu, F. Banat, A. A. Durrani, M. A. Haija, Intrinsically superhydrophobic PVDF membrane by phase inversion for membrane distillation, *Desalination*, 417 (2017) 77–86. <http://dx.doi.org/10.1016/j.desal.2017.05.019>
- [76] S. K. Hubadillah, Z. S. Tai, M. H. D. Othman, Z. Harun, M. R. Jamalludin, M. A. Rahman, J. Jaafar, A. F. Ismail, Hydrophobic ceramic membrane for membrane distillation: A mini review on preparation, characterization, and applications, *Sep. Purif. Technol.* 217 (2019) 71–84. <https://doi.org/10.1016/j.seppur.2019.02.014>
- [77] A. Larbot, L. Gazagnes, S. Krajewski, M. Bukowska, K. Wojciech, Water desalination using ceramic membrane distillation, *Desalination*, 168 (2004) 367–372. <https://doi.org/10.1016/j.desal.2004.07.021>
- [78] H. Fang, J. F. Gao, H. T. Wang, C. S. Chen, Hydrophobic porous alumina hollow fiber for water desalination via membrane distillation process, *J. Membr. Sci.* 403–404 (2012) 41–46. <https://doi.org/10.1016/j.memsci.2012.02.011>
- [79] H. Ramlow, R. K. M. Ferreira, C. Marangoni, R. A. F. Machado, Ceramic membranes applied to membrane distillation: A comprehensive review, *Int. J. Appl. Ceram. Technol.* 16 (2019) 2161–2172. <https://doi.org/10.1111/ijac.13301>
- [80] B. Bolto, J. Zhang, X. Wu, Z. Xie, A Review on Current Development of Membranes for Oil Removal from Wastewaters, *Membranes*, 10 (2020) 65. <https://doi.org/10.3390/membranes10040065>
- [81] Z. Q. Dong, X.-h. Ma, Z. L. Xu, W.-T. You, F. b. Li, Superhydrophobic PVDF–PTFE electrospun nanofibrous membranes for desalination by vacuum membrane distillation, *Desalination*, 347 (2014) 175–183. <https://doi.org/10.1016/j.desal.2014.05.015>
- [82] Y. Shao, M. Han, Y. Wang, G. Li, W. Xiao, X. Li, X. Wu, X. Ruan, X. Yan, G. He, X. Jiang, Superhydrophobic polypropylene membrane with fabricated antifouling interface for vacuum membrane distillation treating high concentration sodium/magnesium saline water, *J. Membr. Sci.* 579 (2019) 240–252. <https://doi.org/10.1016/j.memsci.2019.03.007>
- [83] X. Tan, D. Rodrigue, A review on porous polymeric membrane preparation. Part ii: Production techniques with polyethylene, polydimethylsiloxane, polypropylene, polyimide, and polytetrafluoroethylene, *Polymers*, 11 (2019) 1310. <https://doi.org/10.3390/polym11081310>
- [84] D. Hou, D. Lin, C. Ding, D. Wang, J. Wang, Fabrication and characterization of electrospun superhydrophobic PVDF-HFP/SiNPs hybrid membrane for membrane distillation, *Sep. Purif. Technol.* 189 (2017) 82–89. <https://doi.org/10.1016/j.seppur.2017.07.082>
- [85] F. E. Ahmed, B. S. Lalia, R. Hashaikeh, A review on electrospinning for membrane fabrication: challenges and applications, *Desalination*, 356 (2015) 15–30. <https://doi.org/10.1016/j.desal.2014.09.033>
- [86] W. Ma, Q. Zhang, D. Hua, R. Xiong, J. Zhao, W. Rao, S. Huang, X. Zhan, F. Chen, C. Huang, Electrospun fibers for oil–water separation, *RSC Adv.* 6 (2016) 12868–12884. <https://doi.org/10.1039/C5RA27309A>
- [87] H. Maab, L. Francis, A. Al-Saadi, C. Aubry, N. Ghaffour, G. Amy, S. P. Nunes, Synthesis and fabrication of nanostructured hydrophobic polyazole membranes for low-energy water recovery, *J. Membr. Sci.* 423 (2012) 11–19. <https://doi.org/10.1016/j.memsci.2012.07.009>
- [88] L.-F. Ren, F. Xia, J. Shao, X. Zhang, J. Li, Experimental investigation of the effect of electrospinning parameters on properties of superhydrophobic PDMS/PMMA membrane and its application in membrane distillation, *Desalination*, 404 (2017) 155–166. <https://doi.org/10.1016/j.desal.2016.11.023>
- [89] S. H. Park, S. M. Lee, H. S. Lim, J. T. Han, D. R. Lee, H. S. Shin, Y. Jeong, J. Kim, J. H. Cho, Robust superhydrophobic mats based on electrospun crystalline nanofibers combined with a silane precursor, *ACS Appl. Mater. Interfaces*, 2 (2010) 658–662. <https://doi.org/10.1021/am100005x>
- [90] N. Zhan, Y. Li, C. Zhang, Y. Song, H. Wang, L. Sun, Q. Yang, X. Hong, A novel multinozzle electrospinning process for preparing superhydrophobic PS films with controllable bead-on-string/microfiber morphology, *J. Colloid Interf. Sci.* 345 (2010) 491–495. <https://doi.org/10.1016/j.jcis.2010.01.051>
- [91] X. Li, B. Ding, J. Lin, J. Yu, G. Sun, Enhanced mechanical properties of superhydrophobic microfibrous polystyrene mats via polyamide 6 nanofibers, *J. Phys. Chem.* 113 (2009) 20452–20457. <https://doi.org/10.1021/jp9076933>
- [92] P. Muthiah, S.-H. Hsu, W. Sigmund, Coaxially Electrospun PVDF–Teflon AF and Teflon AF–PVDF Core–Sheath Nanofiber Mats with Superhydrophobic Properties, *Langmuir*, 26 (2010) 12483–12487. <https://doi.org/10.1021/la100748g>
- [93] A. Rosli, A. L. Ahmad, S. C. Low, Anti-wetting polyvinylidene fluoride membrane incorporated with hydrophobic polyethylene-functionalized-silica to improve CO₂ removal in membrane gas absorption, *Sep. Purif. Technol.* 221 (2019) 275–285. <https://doi.org/10.1016/j.seppur.2019.03.094>
- [94] H. P. Ngang, A. L. Ahmad, S. C. Low, B. S. Ooi, Preparation of thermoresponsive PVDF/SiO₂-PNIPAM mixed matrix membrane for saline oil emulsion separation and its cleaning efficiency, *Desalination*, 408 (2017) 1–12. <https://doi.org/10.1016/j.desal.2017.01.005>
- [95] H. Attia, D. J. Johnson, C. J. Wright, N. Hilal, Robust superhydrophobic electrospun membrane fabricated by combination of electrospinning and electrospaying techniques for air gap membrane distillation, *Desalination*, 446 (2018) 70–82. <https://doi.org/10.1016/j.desal.2018.09.001>

- [96] J. Zhang, Z. Song, B. Li, Q. Wang, S. Wang, Fabrication and characterization of superhydrophobic poly (vinylidene fluoride) membrane for direct contact membrane distillation, *Desalination*, 324 (2013) 1–9. <http://dx.doi.org/10.1016/j.desal.2013.05.018>
- [97] L. N. Nthunya, L. Gutierrez, A. R. Verliefe, S. D. Mhlanga, Enhanced flux in direct contact membrane distillation using superhydrophobic PVDF nanofiber membranes embedded with organically modified SiO₂ nanoparticles, *J. Chem. Technol. Biotechnol.* (2019) <https://doi.org/10.1002/jctb.6104>
- [98] Y. Liao, R. Wang, A. G. Fane, Engineering superhydrophobic surface on poly (vinylidene fluoride) nanofiber membranes for direct contact membrane distillation, *J. Membr. Sci.* 440 (2013) 77–87. <https://doi.org/10.1016/j.memsci.2013.04.006>
- [99] Z. Zhu, Y. Liu, H. Hou, W. Shi, F. Qu, F. Cui, W. Wang, Dual-bioinspired design for constructing membranes with superhydrophobicity for direct contact membrane distillation, *Environ. Sci. Technol.* 52 (2018) 3027–3036. <https://doi.org/10.1021/acs.est.7b06227>
- [100] E.-J. Lee, A. K. An, T. He, Y. C. Woo, H. K. Shon, Electrospun nanofiber membranes incorporating fluorosilane-coated TiO₂ nanocomposite for direct contact membrane distillation, *J. Membr. Sci.* 520 (2016) 145–154. <https://doi.org/10.1016/j.memsci.2016.07.019>
- [101] Y. Zhu, J. C. Zhang, J. Zhai, Y. M. Zheng, L. Feng, L. Jiang, Multifunctional carbon nanofibers with conductive, magnetic and superhydrophobic properties, *Chem. Phys. Chem.* 7 (2006) 336–341. <https://doi.org/10.1002/cphc.200500407>
- [102] W. Qing, J. Wang, X. Ma, Z. Yao, Y. Feng, X. Shi, F. Liu, P. Wang, C. Y. Tang, One-Step Tailoring Surface Roughness and Surface Chemistry to Prepare Superhydrophobic Polyvinylidene Fluoride (PVDF) Membranes for Enhanced Membrane Distillation Performances, *J. Colloid Interf. Sci.* 553 (2019) 99–107. <https://doi.org/10.1016/j.jcis.2019.06.011>
- [103] N. F. Himma, N. Prasetya, S. Anisah, I. G. Wenten, Superhydrophobic membrane: progress in preparation and its separation properties, *Rev. Chem. Eng.* 35 (2019) 211–238. <https://doi.org/10.1515/revce-2017-0030>
- [104] S. S. Latthe, A. B. Gurav, C. S. Maruti, R. S. Vhatkar, Recent progress in preparation of superhydrophobic surfaces: a review, *J. Surf. Eng. Mater. Adv. Technol.* 2 (2012) 76. <http://dx.doi.org/10.4236/jsemat.2012.22014>
- [105] S. H. Lee, Z. R. Dilworth, E. Hsiao, A. L. Barnette, M. Marino, J. H. Kim, J.-G. Kang, T.-H. Jung, S. H. Kim, One-step production of superhydrophobic coatings on flat substrates via atmospheric Rf plasma process using non-fluorinated hydrocarbons, *ACS Appl. Mater. Interfaces.* 3 (2011) 476–481. <https://doi.org/10.1021/am101052z>
- [106] S.-H. Lin, K.-L. Tung, W.-J. Chen, H.-W. Chang, Absorption of carbon dioxide by mixed piperazine–alkanolamine absorbent in a plasma-modified polypropylene hollow fiber contactor, *J. Membr. Sci.* 333 (2009) 30–37. <https://doi.org/10.1016/j.memsci.2009.01.039>
- [107] M. M. Puppolo, J. R. Hughey, B. Weber, T. Dillon, D. Storey, E. Cerkez, S. Jansen-Varnum, Plasma modification of microporous polymer membranes for application in biomimetic dissolution studies, *AAPS Open.* 3 (2017) 9. <https://doi.org/10.1186/s41120-017-0019-4>
- [108] J. P. Youngblood, T. J. McCarthy, Ultrahydrophobic polymer surfaces prepared by simultaneous ablation of polypropylene and sputtering of poly (tetrafluoroethylene) using radio frequency plasma, *Macromolecules.* 32 (1999) 6800–6806. <https://doi.org/10.1021/ma9903456>
- [109] J. A. Franco, S. E. Kentish, J. M. Perera, G. W. Stevens, Poly (tetrafluoroethylene) sputtered polypropylene membranes for carbon dioxide separation in membrane gas absorption, *Ind. Eng. Chem. Res.* 50 (2011) 4011–4020. <https://doi.org/10.1021/ie200335a>
- [110] J. A. Franco, S. E. Kentish, J. M. Perera, G. W. Stevens, Fabrication of a superhydrophobic polypropylene membrane by deposition of a porous crystalline polypropylene coating, *J. Membr. Sci.* 318 (2008) 107–113. <https://doi.org/10.1016/j.memsci.2008.02.032>
- [111] H. Ji, G. Chen, J. Hu, X. Yang, C. Min, Y. Zhao, Fabrication of a stable superhydrophobic polypropylene surface by utilizing acetone as a non-solvent, *J. Disper. Sci. and Technol.* 34 (2013) 134–139. <https://doi.org/10.1080/01932691.2011.629518>
- [112] Y. Lv, X. Yu, J. Jia, S.-T. Tu, J. Yan, E. Dahlquist, Fabrication and characterization of superhydrophobic polypropylene hollow fiber membranes for carbon dioxide absorption, *Appl. Energy.* 90 (2012) 167–174. <https://doi.org/10.1016/j.apenergy.2010.12.038>
- [113] H. Y. Erbil, A. L. Demirel, Y. Avci, O. Mert, Transformation of a simple plastic into a superhydrophobic surface, *Science.* 299 (2003) 1377–1380. <https://doi.org/10.1126/science.1078365>
- [114] X. Lu, C. Zhang, Y. Han, Low-density polyethylene superhydrophobic surface by control of its crystallization behavior, *Macromol. Rapid Commun.* 25 (2004) 1606–1610. <https://doi.org/10.1002/marc.200400256>
- [115] X. Li, G. Chen, Y. Ma, L. Feng, H. Zhao, L. Jiang, F. Wang, Preparation of a super-hydrophobic poly (vinyl chloride) surface via solvent–nonsolvent coating, *Polymer.* 47 (2006) 506–509. <https://doi.org/10.1016/j.polymer.2005.08.097>
- [116] C.-H. Xue, S.-T. Jia, J. Zhang, J.-Z. Ma, Large-area fabrication of superhydrophobic surfaces for practical applications: an overview, *Sci. Technol. Adv. Mat.* 11 (2010) 033002. <https://doi.org/10.1088/1468-6996/11/3/033002>
- [117] G. F. Li, X. D. Sun, Y. Z. Zhang, Fabrication of Super-Hydrophobic Membrane with Hydrophilic Polyethersulphone, *Adv. Mater. Res.* 396 (2012) 361–366. <https://doi.org/10.4028/www.scientific.net/AMR.396-398.361>
- [118] S. Raveshyian, R. Yegani, B. Pourabbas, A. Tavakkoli, Study on the fabrication of superhydrophobic microporous polypropylene flat membrane using in situ synthesis of modified fluorinated silica nano particles, *Adv. Mater. Res.* 829 (2014) 371–375. <https://doi.org/10.4028/www.scientific.net/AMR.829.371>
- [119] S. Meng, J. Mansouri, Y. Ye, V. Chen, Effect of templating agents on the properties and membrane distillation performance of TiO₂-coated PVDF membranes, *J. Membr. Sci.* 450 (2014) 48–59. <https://doi.org/10.1016/j.memsci.2013.08.036>
- [120] R. Lakshmi, T. Bharathidasan, P. Bera, B. J. Basu, Fabrication of superhydrophobic and oleophobic sol–gel nanocomposite coating, *Surf. Coat. Technol.* 206 (2012) 3888–3894. <https://doi.org/10.1016/j.surfcoat.2012.03.044>
- [121] S. Liu, X. Liu, S. S. Latthe, L. Gao, S. An, S. S. Yoon, B. Liu, R. Xing, Self-cleaning transparent superhydrophobic coatings through simple sol–gel processing of fluoroalkylsilane, *Appl. Surf. Sci.* 351 (2015) 897–903. <https://doi.org/10.1016/j.apsusc.2015.06.016>
- [122] FAO, The State of World Fisheries and Aquaculture 2018–Meeting the sustainable development goals, Rome, Italy, 2018.
- [123] T. R. Johnson, K. Beard, D. C. Brady, C. J. Byron, C. Cleaver, K. Duffy, N. Keeney, M. Kimble, M. Miller, S. Moeykens, A Social-Ecological System Framework for Marine Aquaculture Research, *Sustainability.* 11 (2019) 2522. <https://doi.org/10.3390/su11092522>
- [124] C. E. Boyd, H. Schmittou, Achievement of sustainable aquaculture through environmental management, *Aquacult. Econ. Manage.* 3 (1999) 59–69. <http://dx.doi.org/10.1080/13657309909380233>
- [125] N. Ahmed, S. Thompson, M. Glaser, Global aquaculture productivity, environmental sustainability, and climate change adaptability, *Environ. Manage.* 63 (2019) 159–172. <https://doi.org/10.1007/s00267-018-1117-3>
- [126] F. E. Dierberg, W. Kiattisimkul, Issues, impacts, and implications of shrimp aquaculture in Thailand, *Environ. Manage.* 20 (1996) 649–666. <https://doi.org/10.1007/BF01204137>
- [127] H. J. Pine, C. E. Boyd, Stream Salinization by Inland Brackish-Water Aquaculture, *N. Am. J. Aquac.* 73 (2011) 107–113. <https://doi.org/10.1080/15222055.2011.545580>
- [128] S. A. Castine, A. D. McKinnon, N. A. Paul, L. A. Trott, R. de Nys, Wastewater treatment for land-based aquaculture: improvements and value-adding alternatives in model systems from Australia, *Aquacult. Environ. Interac.* 4 (2013) 285–300. <https://doi.org/10.3354/aei00088>
- [129] A. Turcios, J. Papenbrock, Sustainable treatment of aquaculture effluents—what can we learn from the past for the future?, *Sustainability.* 6 (2014) 836–856. <https://doi.org/10.3390/su6020836>
- [130] A. B. Dauda, A. Ajadi, A. S. Tola-Fabunmi, A. O. Akinwale, Waste production in aquaculture: Sources, components and managements in different culture systems, *Aquacult. Fish.* 4 (2019) 81–88. <https://doi.org/10.1016/j.aaf.2018.10.002>
- [131] S. Siddiqui, Wastewater treatment technology in aquaculture, *World Aquacult.*, 2003, pp. 49–52.
- [132] J. Davidson, N. Helwig, S. T. Summerfelt, Fluidized sand biofilters used to remove ammonia, biochemical oxygen demand, total coliform bacteria, and suspended solids from an intensive aquaculture effluent, *Aquacult. Eng.* 39 (2008) 6–15. <https://doi.org/10.1016/j.aquaeng.2008.04.002>
- [133] N. a. Ali, N. A. Hanid, A. Jusoh, The potential of a polysulfone (PSF) nanofiltration membrane as the end stage treatment technology of aquaculture wastewater, *Desalin. Water Treat.* 32 (2011) 242–247. <http://dx.doi.org/10.5004/dwt.2011.2706>
- [134] A. Amirkolaie, Environmental impact of nutrient discharged by aquaculture waste water on the Haraz River, *J. Fish. Aquat. Sci.* 3 (2008) 275–279. <https://doi.org/10.3923/jfas.2008.275.279>
- [135] C. Boyd, *Aquaculture Effluents and Water Pollution*, 2011.
- [136] B. O. Omityoin, E. K. Ajani, O. I. Okeleye, B. U. Akpoilih, A. A. Ogunjobi, Biological Treatments of Fish Farm Effluent and its Reuse in the Culture of Nile Tilapia (*Oreochromis niloticus*), *J. Aquac. Res. Dev.* 8 (2017) 1–9. <https://doi.org/10.4172/2155-9546.1000469>
- [137] S. E. Yeo, Binkowski, Frederick P., J. E. Morris, Aquaculture Effluents and Waste By-Products Characteristics, Potential Recovery, and Beneficial Reuse, *NCRAC Technical Bulletins*, 2004.
- [138] A. Coldebella, L. A. Gentelini, A. P. Piana, F. P. Coldebella, R. W. Boscolo, A. Feiden, Effluents from Fish Farming Ponds: A View from the Perspective of Its Main Components, *Sustainability.* 10 (2018) <https://doi.org/10.3390/su10010003>
- [139] G. Qin, C. C. Liu, N. H. Richman, J. E. Moncur, Aquaculture wastewater treatment and reuse by wind-driven reverse osmosis membrane technology: a pilot study on Coconut Island, Hawaii, *Aquacult. Eng.* 32 (2005) 365–378. <https://doi.org/10.1016/j.aquaeng.2004.09.002>
- [140] A. Nora'aini, A. W. Mohammad, A. Jusoh, M. Hasan, N. Ghazali, K. Kamaruzaman, Treatment of aquaculture wastewater using ultra-low pressure asymmetric polyethersulfone (PES) membrane, *Desalination.* 185 (2005) 317–326. <https://doi.org/10.1016/j.desal.2005.03.084>
- [141] J. J. Boccanfuso, E. O. Ariztizabal Abud, M. Berrueta, Improvement of natural spawning of black flounder, *Paralichthys orbignyanus* (Valenciennes, 1839) by photothermal and salinity conditioning in recirculating aquaculture system, *Aquaculture.* 502 (2019) 134–141. <https://doi.org/10.1016/j.aquaculture.2018.12.034>
- [142] Y. Tsuda, W. Sakamoto, S. Yamamoto, O. Murata, Effect of environmental fluctuations on mortality of juvenile Pacific bluefin tuna, *Thunnus orientalis*, in closed life-cycle aquaculture, *Aquaculture.* 330–333 (2012) 142–147. <https://doi.org/10.1016/j.aquaculture.2011.12.008>
- [143] D. Yang, W. Yu, Z. Miao, M. Li, Y. Zhou, Environmental changing characteristics

- of offshore cage aquaculture area in Yueqing Bay, 2014 IEEE Workshop on Electronics, Computer and Applications. (2014) 999-1001. <https://doi.org/10.1109/IWECA.2014.6845791>
- [144] M. J. Resley, K. A. Webb, G. J. Holt, Growth and survival of juvenile cobia, *Rachycentron canadum*, at different salinities in a recirculating aquaculture system, *Aquaculture*. 253 (2006) 398-407. <https://doi.org/10.1016/j.aquaculture.2005.08.023>
- [145] R W. Hickman, P. Redfearn, M.J. Tait, Novel effects of salinity and water reuse on growth of juvenile New Zealand turbot, *Colistium nudipinnis* (Waite 1910), a potential aquaculture species, *Aquac. Res.* 33 (2002) 1009-1018. <https://doi.org/10.1046/j.1365-2109.2002.00758.x>
- [146] A. Ozaki, P. Kaewjantawee, M. Anongponyoskul, N. V. Thinh, M. Matsumoto, M. Harada, K. Hamagami, T. Okayasu, Heat storage induced by salinity stratification in tropical saline aquaculture ponds, 2019 ASABE Annual International Meeting. (2019) 1. <https://doi.org/10.13031/aim.201901005>